



This is a repository copy of *Cramr-Rao bound analysis of underdetermined wideband DOA estimation under the subband model via frequency decomposition*.

White Rose Research Online URL for this paper:  
<https://eprints.whiterose.ac.uk/175154/>

Version: Accepted Version

---

**Article:**

Liang, Y., Cui, W., Shen, Q. et al. (2 more authors) (2021) Cramr-Rao bound analysis of underdetermined wideband DOA estimation under the subband model via frequency decomposition. *IEEE Transactions on Signal Processing*, 69. pp. 4132-4148. ISSN 1053-587X

<https://doi.org/10.1109/tsp.2021.3088231>

---

© 2021 IEEE. Personal use of this material is permitted. Permission from IEEE must be obtained for all other users, including reprinting/ republishing this material for advertising or promotional purposes, creating new collective works for resale or redistribution to servers or lists, or reuse of any copyrighted components of this work in other works. Reproduced in accordance with the publisher's self-archiving policy.

**Reuse**

Items deposited in White Rose Research Online are protected by copyright, with all rights reserved unless indicated otherwise. They may be downloaded and/or printed for private study, or other acts as permitted by national copyright laws. The publisher or other rights holders may allow further reproduction and re-use of the full text version. This is indicated by the licence information on the White Rose Research Online record for the item.

**Takedown**

If you consider content in White Rose Research Online to be in breach of UK law, please notify us by emailing [eprints@whiterose.ac.uk](mailto:eprints@whiterose.ac.uk) including the URL of the record and the reason for the withdrawal request.



[eprints@whiterose.ac.uk](mailto:eprints@whiterose.ac.uk)  
<https://eprints.whiterose.ac.uk/>

# Cramér-Rao Bound Analysis of Underdetermined Wideband DOA Estimation Under the Subband Model via Frequency Decomposition

Yibao Liang, Wei Cui, Qing Shen, Wei Liu, *Senior Member, IEEE*, Siliang Wu

**Abstract**—A class of Cramér-Rao bounds (CRBs) for wideband direction-of-arrival (DOA) estimation under the subband (or frequency bin) model is studied for the underdetermined case, where the number of sources is no less than that of physical sensors. A unified framework is proposed to encompass the closed-form CRB expressions for DOAs in four cases where the sources are known *a priori* to 1) have flat spectra/cross spectra, 2) be spatially uncorrelated, 3) be spatially uncorrelated and have proportional spectra up to unknown factors, 4) be spatially uncorrelated and have flat spectra. The relationship between the wideband CRBs and the subband ones is investigated, and the order relationship among the derived CRBs are provided. The asymptotic behavior of the CRBs with respect to the number of snapshots and the signal-to-noise ratio (SNR) is discussed. Two asymptotic expressions for sufficiently large SNR are derived in both overdetermined and underdetermined cases. Existence of the derived CRBs is examined through rank conditions of the introduced matrices, which yields upper bounds on the resolution capacities. Different from the narrowband scenario, underdetermined wideband DOA estimation is feasible even if a sparse array is not used given different *a priori* knowledge about the source spectra. It is possible to resolve more wideband Gaussian sources than the number of DOFs offered by the difference co-array. Finally, further interpretations of the subband model are provided, revealing the underlying connections with the multi-frequency co-array augmentation concept and the non-coherent subarray system.

**Index Terms**—Cramér-Rao bound, direction-of-arrival estimation, wideband, subband model, underdetermined.

## I. INTRODUCTION

**D**IRECTION of arrival (DOA) estimation is a fundamental topic in array signal processing, which has been extensively studied over the past decades. A plethora of methods and algorithms have been developed for the narrowband DOA estimation problem, and the Cramér-Rao bound (CRB) has been systematically studied for both deterministic and stochastic models [2]–[4].

Different from the narrowband scenario, mathematically the array sampling process for wideband signals involves

This paper was presented in part at the IEEE Global Conference on Signal and Information Processing (GlobalSIP), Ottawa, Canada, Nov. 2019 [1]. This work was supported in part by the National Natural Science Foundation of China under Grants 61801028 and 61628101, and in part by the Beijing Institute of Technology Research Fund Program for Young Scholars. (Corresponding author: Qing Shen.)

Y. Liang, W. Cui, Q. Shen, and S. Wu are with the School of Information and Electronics, Beijing Institute of Technology, Beijing, 100081, China (e-mail: liangyibao@bit.edu.cn, cuiwei@bit.edu.cn, qing-shen@outlook.com, siliangw@bit.edu.cn).

W. Liu is with the Department of Electronic and Electrical Engineering, University of Sheffield, Sheffield, S1 3JD, UK (e-mail: w.liu@sheffield.ac.uk).

matrix convolution instead of direct multiplication [5], [6], and various modeling schemes have been introduced, such as the subband (or frequency bin) model [7], [8], the pole-zero model [5], [9], the frequency-dependent model [10], the harmonic source model [11], the spatial-only model [12], and the spatio-temporal model [6].

In this paper, we focus on the subband model, where the wideband problem is formulated in the spatio-frequency domain. This model is usually established by dividing the temporal observation interval into a group of nonoverlapping subintervals and then applying the discrete Fourier transform (DFT) or, more generally, a filter bank system. Therefore, the processing bandwidth is decomposed into a set of subbands that resemble narrowband settings under proper model assumptions. Based on this subband model, the signal subspace methods [7], [8], [13]–[20] and the maximum likelihood (ML) methods [21]–[24] can be implemented to produce high-resolution DOA estimates. To guarantee unique source identifiability, these classical methods commonly assume that the number of sources is smaller than that of sensors.

In recent years, sparse arrays, such as nested array [25], co-prime array [26]–[28], and their extensions [29]–[33], have attracted much research interest. Exploiting the enhanced degrees of freedoms (DOFs) offered by the virtual co-array, effective techniques such as the spatial smoothing (SS) based methods [25], the compressive sensing (CS) based methods [34], and the ML methods [35] can be applied to resolve more sources than the number of physical sensors. This has provided an incentive to develop underdetermined wideband algorithms. The SS-based methods [36], [37] and the CS-based methods [37]–[42] have been successfully extended to the subband model, which can resolve many more sources than classical algorithms.

To assess the performance of various algorithms developed for the subband model, an appropriate statistical tool is necessary. Since the Fourier coefficients at each subband share similar statistical characteristics with the temporal samples in narrowband settings, the narrowband CRB can be extended to yield a “wideband CRB”. This CRB establishes the baseline for the variance of any unbiased estimator using the covariance matrix of the frequency domain samples, which is a sufficient statistic for the wideband Gaussian problem under the condition that the frequency domain samples at different subbands are uncorrelated [43]. Note that the wideband CRB derived in this way corresponds to the subband model, and it is different from the CRBs for other models, e.g., [5], [44].

Since the deterministic CRB does not exist in the underdetermined case [45], we shall concentrate on the stochastic CRB. Initially, this CRB was evaluated numerically from the Fisher information matrix (FIM) [8], [46], [47]. In [21], a closed-form expression for the small-error variance of the deterministic ML estimator was derived, which serves as an approximation to the stochastic CRB. Then, another approximate CRB expression for two uncorrelated, closely-spaced sources was reported in [48]. The closed-form expression for the stochastic CRB associated with the DOAs was first presented in [49]. Validity of this CRB expression indicates that the number of resolvable sources is less than the number of physical sensors under the general subband model. Through numerical comparisons among the CRBs with different *a priori* knowledge about the source spectra in the dual-source case, Messer has found that the performance gain brought by different *a priori* knowledge is potentially significant in rather limited conditions, and in particular, an intermediate CRB expression was derived [43]. The CRB analyses outlined above are conducted in the overdetermined case only, and underdetermined estimation is feasible only if some *a priori* knowledge about the signals is available.

In literature, there are four types of *a priori* knowledge considered for the wideband case by different researchers:

$\mathcal{P}_f$ : The spectra/cross spectra of the sources are *flat* at the subbands of interest.

$\mathcal{P}_u$ : The sources are spatially *uncorrelated*.

$\mathcal{P}_{up}$ : The sources are spatially *uncorrelated*, and their spectra are *proportional* up to unknown factors at the subbands of interest.

$\mathcal{P}_{uf}$ : The sources are spatially *uncorrelated*, and their spectra are *flat* at the subbands of interest.

In practice,  $\mathcal{P}_f$  is available when all the lagged data correlation matrices have approximately the same information, such as acoustic backscattered signals from an underwater target [50].  $\mathcal{P}_f$  has been introduced in some celebrated algorithms [44], [51] and theoretical studies [43], [49].  $\mathcal{P}_u$  is available when the propagation channel is unbounded [13], [43], and it is adopted by most wideband underdetermined DOA estimation algorithms [36]–[38], [40], [41], [52].  $\mathcal{P}_{up}$  is available in cases such as a wireless communication system where all sources use the same modulation format and pulse shaping functions [53]. Recently, two underdetermined DOA estimation algorithms using sparse arrays were developed based on  $\mathcal{P}_{up}$  [54], [55]. In addition,  $\mathcal{P}_{uf}$  has also attracted a lot of interest, with a number of algorithms [12], [46] and theoretical studies [43], [56] reported.

Due to the inherited overdetermined model assumption, existing results on the wideband stochastic CRB are not suitable to assess the performance of underdetermined algorithms. To bridge the gap between the CRB and existing algorithms employing  $\mathcal{P}_u$ , a closed-form CRB expression has been derived in our conference paper [1], but closed-form CRB expressions with other popular *a priori* knowledge are still unavailable. So far, only  $\mathcal{P}_u$  has found wide applications in underdetermined DOA estimation methods. Most algorithms employing  $\mathcal{P}_f$  are not developed for the underdetermined case, even though such

an application is theoretically feasible [43], [49], [56]. The emergence of a very recent wideband DOA estimation method exploiting  $\mathcal{P}_{up}$  [55] implies that popular *a priori* knowledge will inspire more underdetermined DOA estimation techniques in the future. In short, the potential for underdetermined DOA estimation using different *a priori* knowledge has not been well-understood and deserves further investigation.

*Motivation:* In contrast to the variety of algorithms based on the subband model, existing results on the wideband stochastic CRB are somewhat scanty and limited to the overdetermined case. The first objective of this paper is to extend our previous work in [1] and conduct a more comprehensive study on the stochastic CRBs with different *a priori* knowledge. This will provide useful tools to analyze the performance of existing and future DOA estimation methods, especially in the underdetermined case. Moreover, as early CRB results offer limited insights into the underdetermined problem, it is important to study how the resolution capacity can be improved by employing different *a priori* knowledge.

*Organization and Contributions:* The rest of this paper is organized as follows. The stochastic Gaussian subband model is introduced in Section II. The subsequent sections present the main contributions as summarized below.

- The general formula for the wideband stochastic CRB is reviewed, and a unified framework for the DOA-related block of the CRB is directly derived. This framework encompasses four closed-form CRB expressions in the four cases with  $\mathcal{P}_f$ ,  $\mathcal{P}_u$ ,  $\mathcal{P}_{up}$ , and  $\mathcal{P}_{uf}$  (Section III). Compared with the existing wideband CRB results for the overdetermined case [43], [49], our derived CRB expressions are written in closed-forms and applicable to the underdetermined case.
- The relationship between the wideband CRBs and the subband ones is investigated, connecting our CRB with the existing narrowband one [57]. Then, the order relationship among the CRBs are proved. The asymptotic behavior of the CRBs with respect to the number of snapshots and the signal-to-noise ratio (SNR) is investigated, with two asymptotic CRB expressions derived for sufficiently large SNR. With the increase of SNR, the wideband CRB approaches to zero in the overdetermined case, while in contrast, it converges to a positive constant in the underdetermined case. The conditions under which our derived CRBs exist are demonstrated by the rank conditions of the introduced matrices (Section IV).
- The upper bounds on the resolution capacities in different cases are derived based on the rank conditions. For linear arrays, the possibility for underdetermined DOA estimation is discussed through a detailed examination of the existence of the CRBs. It is found that the subband model itself can provide enhanced DOFs for underdetermined DOA estimation, while the assistance of a sparse array is not indispensable. Moreover, more wideband Gaussian sources than narrowband ones can be resolved based on a given linear array, either uniform or sparse. By employing  $\mathcal{P}_{up}$  or  $\mathcal{P}_{uf}$ , it is possible to resolve more wideband Gaussian sources than the number of DOFs offered by the difference co-array. Further interpretations

of the subband model is presented, revealing connections with the multi-frequency co-array argumentation concept and the non-coherent subarray system (Section V).

Simulations are given in Section VI, and conclusions are drawn in Section VII.

*Notations:* Matrices are represented by bold uppercase letters, such as  $\mathbf{A}$  and  $\mathcal{A}$ . Fourier coefficients are also denoted by bold uppercase letters, such as  $\mathbf{X}$ ,  $\mathbf{S}$ , and  $\mathbf{N}$ . Vectors are represented by bold lowercase letters, such as  $\mathbf{a}$ ,  $\mathbf{r}$ , and  $\mathbf{p}$ . Variables are denoted by non-bold letters, such as  $K$  and  $m$ . The real set, positive real set, and complex set are denoted by  $\mathbb{R}$ ,  $\mathbb{R}_+$ , and  $\mathbb{C}$ , respectively.  $\mathbb{C}^{M \times N}$  is the space of  $M$ -by- $N$  complex-valued matrices. The cardinality of a set  $\mathbb{A}$  is denoted by  $|\mathbb{A}|$ . For a matrix  $\mathbf{A}$ , denote  $\mathbf{A}^*$ ,  $\mathbf{A}^T$ , and  $\mathbf{A}^H$  as its conjugate, transpose, and Hermitian transpose, respectively. The  $(i, j)$ -th element of  $\mathbf{A}$  is  $\langle \mathbf{A} \rangle_{i,j}$ . The real and imaginary parts of  $\mathbf{A}$  are  $\text{Re}(\mathbf{A})$  and  $\text{Im}(\mathbf{A})$ . The trace of a square matrix  $\mathbf{A}$  is  $\text{tr}(\mathbf{A})$ . For a matrix  $\mathbf{A}$  of full column rank, the orthogonal projector onto the null space of  $\mathbf{A}^H$  is  $\Pi_{\mathbf{A}}^\perp = \mathbf{I} - \mathbf{A}(\mathbf{A}^H\mathbf{A})^{-1}\mathbf{A}^H$ .  $\mathbf{I}_M$  is the  $M \times M$  identity matrix. Given  $L$  matrices  $\mathbf{A}_1, \dots, \mathbf{A}_L$ , the block diagonalizing operation is  $\text{blkdiag}(\mathbf{A}_1, \dots, \mathbf{A}_L)$ . The column vectorization of  $\mathbf{A}$  is  $\text{vec}(\mathbf{A})$ . For two Hermitian matrices  $\mathbf{A}$  and  $\mathbf{B}$ , the inequality  $\mathbf{A} \preceq \mathbf{B}$  means that  $\mathbf{A} - \mathbf{B}$  is negative semidefinite.  $\otimes$ ,  $\odot$ , and  $\circ$  stand for the Kronecker product, the Khatri-Rao product, and the Hadamard product, respectively.

## II. SUBBAND MODEL FOR THE WIDEBAND DOA ESTIMATION PROBLEM

Consider an array of  $M$  ( $M > 1$ ) omnidirectional sensors with identical responses. The array receives signals emitted by  $K$  ( $K \geq 1$ ) wideband co-channel sources located at distinct directions  $\boldsymbol{\theta} = [\theta_1, \dots, \theta_K]^T$  in the far field. The output signal at the  $m$ -th sensor can be expressed as

$$\begin{aligned} x_m(t) &= \sum_{k=1}^K s_k[t - \tau_m(\theta_k)] + n_m(t), \\ m &= 1, \dots, M, \quad k = 1, \dots, K, \end{aligned} \quad (1)$$

where  $s_k(t)$  is the signal emitted by the  $k$ -th source,  $\tau_m(\theta_k)$  is the time delay of the signal from angle  $\theta_k$  arriving at the  $m$ -th sensor, and  $n_m(t)$  is the additive noise.

The observation time interval is sampled into  $N$  temporal snapshots by a frequency  $f_s$  and then divided into  $Q$  nonoverlapping subintervals with a duration  $\Delta t$ . Next, an  $L$ -point DFT is applied to each subinterval. Suppose that  $\Delta t$  is much longer than the maximum value of  $\tau_m(\theta_k)$ , so that the propagation time delay approximately corresponds to a phase shift in the Fourier coefficients [7]. This leads to

$$\mathbf{X}_{l,q} = \mathbf{A}_l \mathbf{S}_{l,q} + \mathbf{N}_{l,q}, \quad l = 1, \dots, L, \quad q = 1, \dots, Q, \quad (2)$$

where  $l$  is the index of the subband frequency  $f_l$ .  $\mathbf{X}_{l,q} \in \mathbb{C}^{M \times 1}$ ,  $\mathbf{S}_{l,q} \in \mathbb{C}^{K \times 1}$ , and  $\mathbf{N}_{l,q} \in \mathbb{C}^{M \times 1}$  hold the Fourier coefficients of the array output signals, the source signals and the noise, respectively, for the  $q$ -th subinterval. For the  $l$ -th subband,  $\{\mathbf{X}_{l,q}\}_{q=1}^Q$  can be treated as frequency domain samples. The array manifold matrix is  $\mathbf{A}_l = [\mathbf{a}_{l,1}, \dots, \mathbf{a}_{l,K}]$  with  $\mathbf{a}_{l,k}$  denoting the steering vector associated with the  $l$ -th

subband and the  $k$ -th source. Note that the dependence of  $\mathbf{A}_l$  on the DOAs is dropped for simplicity.

We introduce the following standard assumptions [22], [43].

- The source signals are stationary, zero-mean, stochastic Gaussian, possibly correlated processes, with unknown cross-spectral density matrices (CSDMs)  $\{\mathbf{P}_l\}_{l=1}^L$ .
- The noise is a stationary, zero-mean, stochastic Gaussian, spatially uncorrelated process, independent of the source signals. Its spatial covariance matrix at the  $l$ -th subband is  $\sigma_l \mathbf{I}_M$ , with  $\sigma_l \in \mathbb{R}_+$  being the noise power.
- The number of sources,  $K$ , is known.

Most algorithms do not assume any specific probability distribution for the source signals, but the Gaussian distribution is commonly advocated in performance study mainly for three reasons: 1) the probability density function of the data has a convenient form under the Gaussian distribution, so that the likelihood function and the FIM are mathematically tractable; 2) under rather general conditions and in large samples, the Gaussian CRB is larger than any other CRBs associated with arbitrary congruous distributions [58], so it can be attained with less difficulty and embraces more practical value; 3) the estimation schemes derived from the stochastic Gaussian model has been found to yield superior performance, regardless of the actual distribution of emitter signals [59]. Nonetheless, the Gaussian assumption can be relaxed. According to the central limit theorem, the Fourier coefficients are asymptotically independently Gaussian distributed when the observation duration is sufficiently long [47], [60].

Let  $l_1$  and  $l_2$  represent two distinct subband indices. Let  $\mathbf{R}_l$  and  $\mathbf{R}_{l_1, l_2}$  denote the auto-covariance matrix of  $\mathbf{X}_l$  and the cross-covariance matrix of  $\mathbf{X}_{l_1}$  and  $\mathbf{X}_{l_2}$ , respectively. In practice, they can be estimated by  $\hat{\mathbf{R}}_l = 1/Q \sum_{q=1}^Q \mathbf{X}_{l,q} \mathbf{X}_{l,q}^H$  and  $\hat{\mathbf{R}}_{l_1, l_2} = 1/Q \sum_{q=1}^Q \mathbf{X}_{l_1, q} \mathbf{X}_{l_2, q}^H$ , and together serve as sufficient statistics for the wideband Gaussian problem [43]. Although  $\mathbf{R}_{l_1, l_2}$  is useful for some algorithms [39], [41], [42], most estimators are derived based on a consistent and unbiased estimate of  $\mathbf{R}_l$  [19]. The correlation among subbands, together with the edge effect and spectral leakage might break the consistency and lead to biased estimates [6]. To mitigate this, zero padding or windows [61] could be used, but this would remove the orthogonality of the noise component across frequency [24]. This difficulty is often circumvented by introducing the following assumption [7], [19], [21], [43]:

- $\Delta t$  is much larger than the correlation time of the processes involved.

As such,  $\mathbf{X}_{l_1, q}$  and  $\mathbf{X}_{l_2, q}$  are asymptotically uncorrelated, so that  $\mathbf{R}_l$  approximately equals the CSDM [7]. Thus,

$$\mathbf{R}_l = \mathbf{A}_l \mathbf{P}_l \mathbf{A}_l^H + \sigma_l \mathbf{I}_M. \quad (3)$$

The CRB derived under this assumption is an approximation of the truth, but is of practical value since most algorithms use  $\hat{\mathbf{R}}_l$  as the actual measured data [43].

As the source number is assumed to be known, so is the number of unknown DOAs, it reduces part of the modeling uncertainty. The assumed uncorrelatedness among different subbands not only eliminates the unknown parameters in  $\mathbf{R}_{l_1, l_2}$ , but also alludes to a rough knowledge, i.e., smoothness,

about the signal spectra. This knowledge implies that one only needs to estimate a subset of subbands rather than all of them [43], [49]. To avoid overparameterization, order selection rules [58] could be applied simultaneously with DOA estimation techniques, but this would be computationally intensive. The unknown-order CRB could be calculated from the formula in [62], but it also depends on a specific order selection rule. However, most algorithms do not include an order selection rule but still obtain high-resolution estimates using a subset of subbands, as if the true model order for the signal spectra is known and can be correctly characterized by these subbands, while the other ones are ignored. To derive a practical CRB that evaluates the statistical efficiency of such estimators, only the subbands of interest shall be considered.

### III. UNIFIED FRAMEWORK FOR THE DOA-RELATED BLOCKS OF WIDEBAND STOCHASTIC CRBS

#### A. General Formula for the Wideband Stochastic CRB

Under the established stochastic Gaussian subband model,  $\mathbf{X}_{l_1,q}$  and  $\mathbf{X}_{l_2,q}$  can be treated as asymptotically independent due to the well-known equivalence between uncorrelatedness and independence under joint Gaussian distribution. Redefine  $L$  as the number of subbands of interest and  $l$  their indices. Denote  $\mathbf{F}_l$  as the FIM at the  $l$ -th subband, and then the wideband FIM can be expressed as

$$\tilde{\mathbf{F}} = \sum_{l=1}^L \mathbf{F}_l. \quad (4)$$

Let  $\boldsymbol{\alpha}$  and  $\mathbf{B}(\boldsymbol{\alpha})$  denote the real-valued unknown parameter vector and the CRB for  $\boldsymbol{\alpha}$ , respectively. Note that  $\tilde{\mathbf{F}}$  is nonnegative definite by definition. Assume that  $\tilde{\mathbf{F}}$  is nonsingular, and then  $\mathbf{B}(\boldsymbol{\alpha}) = \tilde{\mathbf{F}}^{-1}$ . According to the Slepian-Bangs formula [63], [64], the  $(i, j)$ -th element of  $\mathbf{B}^{-1}(\boldsymbol{\alpha})$  is given by

$$\langle \mathbf{B}^{-1}(\boldsymbol{\alpha}) \rangle_{i,j} = Q \sum_{l=1}^L \text{tr} \left( \mathbf{R}_l^{-1} \frac{\partial \mathbf{R}_l}{\partial (\boldsymbol{\alpha})_i} \mathbf{R}_l^{-1} \frac{\partial \mathbf{R}_l}{\partial (\boldsymbol{\alpha})_j} \right). \quad (5)$$

Using the following identities [65],

$$\begin{aligned} \text{tr}(\mathbf{A}\mathbf{B}\mathbf{C}\mathbf{D}) &= \text{vec}(\mathbf{B}^H)^H (\mathbf{A}^T \otimes \mathbf{C}) \text{vec}(\mathbf{D}), \\ \text{vec}(\mathbf{A}\mathbf{B}\mathbf{C}) &= (\mathbf{C}^T \otimes \mathbf{A}) \text{vec}(\mathbf{B}), \end{aligned} \quad (6)$$

we can rewrite (5) as

$$\langle \mathbf{B}^{-1}(\boldsymbol{\alpha}) \rangle_{i,j} = Q \sum_{l=1}^L \left( \mathbf{W}_l \frac{\partial \mathbf{r}_l}{\partial (\boldsymbol{\alpha})_i} \right)^H \left( \mathbf{W}_l \frac{\partial \mathbf{r}_l}{\partial (\boldsymbol{\alpha})_j} \right), \quad (7)$$

where

$$\mathbf{W}_l = (\mathbf{R}_l^T \otimes \mathbf{R}_l)^{-\frac{1}{2}}, \quad \mathbf{r}_l = \text{vec}(\mathbf{R}_l). \quad (8)$$

Equation (5) is the extensively studied wideband stochastic CRB formula [8], [43], [47], [49]. However, it does not offer enough analytical insights, so that existing results are mainly obtained through numerical analysis. In many applications, only the DOA-related block is desired [3], while the other unknowns are nuisance parameters.

#### B. Derivation of the Unified CRB Framework

Starting from (7), we aim to derive a closed-form CRB expression for the DOA-related block. The key step is calculating  $\partial \mathbf{r}_l / \partial \boldsymbol{\alpha}^T$ , and we shall investigate four cases where  $\mathcal{P}_f$ ,  $\mathcal{P}_u$ ,  $\mathcal{P}_{\text{up}}$ , and  $\mathcal{P}_{\text{uf}}$  are employed, respectively.

Let the column vector  $\mathbf{p}_l$  collect all the real-valued unknown entries that determine  $\mathbf{P}_l$ . In general, the sources are possibly correlated, and thus  $\mathbf{P}_l$  is determined by  $K^2$  real-valued unknowns associated with the upper triangular entries, yielding

$$\mathbf{p}_l = [\langle \mathbf{P}_l \rangle_{1,1}, \text{Re}(\langle \mathbf{P}_l \rangle_{1,2}), \text{Im}(\langle \mathbf{P}_l \rangle_{1,2}), \dots, \langle \mathbf{P}_l \rangle_{K,K}]^T. \quad (9)$$

It follows from (3) and (6) that  $\mathbf{r}_l$  can be expressed as

$$\mathbf{r}_l = \mathbf{C}_l \boldsymbol{\Psi} \mathbf{p}_l + \sigma_l \mathbf{i}, \quad (10)$$

where  $\mathbf{C}_l = \mathbf{A}_l^* \otimes \mathbf{A}_l$ ,  $\mathbf{i} = \text{vec}(\mathbf{I}_M)$ , and  $\boldsymbol{\Psi} \in \mathbb{R}^{K^2 \times K^2}$  is a nonsingular matrix satisfying [66]

$$\text{vec}(\mathbf{P}_l) = \boldsymbol{\Psi} \mathbf{p}_l. \quad (11)$$

If the sources are known to be uncorrelated ( $\mathcal{P}_u$ ), then  $\mathbf{P}_l$  is a real-valued diagonal matrix, leading to

$$\mathbf{p}_l = [\langle \mathbf{P}_l \rangle_{1,1}, \dots, \langle \mathbf{P}_l \rangle_{K,K}]^T. \quad (12)$$

Different from (10),  $\mathbf{r}_l$  will take another form such that

$$\mathbf{r}_l = \mathbf{D}_l \mathbf{p}_l + \sigma_l \mathbf{i}, \quad (13)$$

where

$$\mathbf{D}_l = \mathbf{A}_l^* \odot \mathbf{A}_l. \quad (14)$$

*Remark 1:* Equations (10) and (13) resemble two single-snapshot deterministic signal representations, where  $\mathbf{C}_l \boldsymbol{\Psi}$  and  $\mathbf{D}_l$  behave as distinct array manifold matrices. In particular,  $\mathbf{D}_l$  is associated with the difference co-array consisting of many more virtual sensors than the physical array. Therefore, most existing underdetermined DOA estimation methods employ  $\mathcal{P}_u$  and exploit the difference co-array to achieve strong source resolvability.

For the unknown parameter vector  $\boldsymbol{\alpha}$ , in general, it consists of DOAs, noise powers, and the real-valued parameters associated with the source covariance matrices, which vary with different *a priori* knowledge.

If  $\mathcal{P}_f$  is employed, we can write  $\{\mathbf{P}_l\}_{l=1}^L = \mathbf{P}_1$  by choosing the first subband as the reference. Using (9), we have

$$\boldsymbol{\alpha} = [\theta_1, \dots, \theta_K, \langle \mathbf{P}_1 \rangle_{1,1}, \text{Re}(\langle \mathbf{P}_1 \rangle_{1,2}), \text{Im}(\langle \mathbf{P}_1 \rangle_{1,2}), \dots, \langle \mathbf{P}_1 \rangle_{K,K}, \sigma_1, \dots, \sigma_K]^T. \quad (15)$$

If  $\mathcal{P}_u$  is employed, it follows from (12) that

$$\boldsymbol{\alpha} = [\theta_1, \dots, \theta_K, \langle \mathbf{P}_1 \rangle_{1,1}, \dots, \langle \mathbf{P}_1 \rangle_{K,K}, \dots, \langle \mathbf{P}_L \rangle_{1,1}, \dots, \langle \mathbf{P}_L \rangle_{K,K}, \sigma_1, \dots, \sigma_K]^T. \quad (16)$$

If  $\mathcal{P}_{\text{up}}$  is employed,  $\{\mathbf{P}_l\}_{l=1}^L$  are proportional and diagonal. Choose the first subband as the reference and let  $l' = 2, \dots, L$ . Then, we can write  $\{\mathbf{P}_{l'}\}_{l'=2}^L = \xi_{l'} \mathbf{P}_1$  with  $\xi_{l'} \in \mathbb{R}_+$  being an unknown proportional factor. In this case,

$$\boldsymbol{\alpha} = [\theta_1, \dots, \theta_K, \langle \mathbf{P}_1 \rangle_{1,1}, \dots, \langle \mathbf{P}_1 \rangle_{K,K}, \xi_2, \dots, \xi_L, \sigma_1, \dots, \sigma_K]^T. \quad (17)$$

If  $\mathcal{P}_{\text{uf}}$  is employed,  $\{\mathbf{P}_l\}_{l=1}^L$  are identical and diagonal. Removing the off-diagonal entries in (15), we obtain

$$\boldsymbol{\alpha} = [\theta_1, \dots, \theta_K, \langle \mathbf{P}_1 \rangle_{1,1}, \dots, \langle \mathbf{P}_1 \rangle_{K,K}, \sigma_1, \dots, \sigma_K]^T. \quad (18)$$

With the above results, we can calculate  $\partial \mathbf{r}_l / \partial \boldsymbol{\alpha}^T$  and substitute it into (7). Although the derivation of a closed-form CRB for each case varies, the final results share a similar form. In the following *Theorem 1*, we provide a unified framework for the closed-form CRB expressions in four cases.

*Theorem 1:* Let  $\mathbf{B}(\boldsymbol{\theta})$  denote the DOA-related block of the wideband stochastic CRB. Assume the wideband FIM is nonsingular, and then the unified framework for  $\mathbf{B}(\boldsymbol{\theta})$  is

$$\mathbf{B}(\boldsymbol{\theta}) = \frac{1}{Q} (\mathbf{G}^H \boldsymbol{\Pi}_{\Delta}^{\perp} \mathbf{G})^{-1}, \quad (19)$$

where  $\mathbf{G}$  is associated with the DOAs, while  $\Delta$  is related to the nuisance parameters. According to the employed *a priori* knowledge,  $\mathbf{G}$  and  $\Delta$  take the following different forms:

If  $\mathcal{P}_f$  is employed, then

$$\mathbf{G} = \begin{bmatrix} \mathbf{w}_1 \bar{\mathbf{C}}_1 \\ \vdots \\ \mathbf{w}_L \bar{\mathbf{C}}_L \end{bmatrix}, \Delta = \begin{bmatrix} \mathbf{w}_1 \mathbf{C}_1 \Psi & \mathbf{w}_1 \mathbf{i} & & \\ & \ddots & \ddots & \\ & & \mathbf{w}_L \mathbf{i} & \end{bmatrix}. \quad (20)$$

If  $\mathcal{P}_u$  is employed, then

$$\mathbf{G} = \begin{bmatrix} \mathbf{w}_1 \bar{\mathbf{D}}_1 \mathbf{P}_1 \\ \vdots \\ \mathbf{w}_L \bar{\mathbf{D}}_L \mathbf{P}_L \end{bmatrix}, \Delta = \begin{bmatrix} \mathbf{w}_1 \mathbf{D}_1 & & & \mathbf{w}_1 \mathbf{i} \\ & \ddots & & \vdots \\ & & \mathbf{w}_L \mathbf{D}_L & \vdots \\ & & & \mathbf{w}_L \mathbf{i} \end{bmatrix}. \quad (21)$$

If  $\mathcal{P}_{\text{up}}$  is employed, then

$$\mathbf{G} = \begin{bmatrix} \mathbf{w}_1 \bar{\mathbf{D}}_1 \mathbf{P}_1 \\ \xi_2 \mathbf{w}_2 \bar{\mathbf{D}}_2 \mathbf{P}_1 \\ \vdots \\ \xi_L \mathbf{w}_L \bar{\mathbf{D}}_L \mathbf{P}_1 \end{bmatrix}, \Delta = \begin{bmatrix} \mathbf{w}_1 \mathbf{D}_1 & 0 & \dots & 0 & \mathbf{w}_1 \mathbf{i} \\ \xi_2 \mathbf{w}_2 \mathbf{D}_2 & \mathbf{w}_2 \mathbf{D}_2 \mathbf{P}_1 & & & \mathbf{w}_2 \mathbf{i} \\ \vdots & & \ddots & & \vdots \\ \xi_L \mathbf{w}_L \mathbf{D}_L & & & \mathbf{w}_L \mathbf{D}_L \mathbf{P}_1 & \mathbf{w}_L \mathbf{i} \end{bmatrix}, \quad (22)$$

with  $\mathbf{p}_1 = [\langle \mathbf{P}_1 \rangle_{1,1}, \dots, \langle \mathbf{P}_1 \rangle_{K,K}]^T$ .

If  $\mathcal{P}_{\text{uf}}$  is employed, then

$$\mathbf{G} = \begin{bmatrix} \mathbf{w}_1 \bar{\mathbf{D}}_1 \mathbf{P}_1 \\ \vdots \\ \mathbf{w}_L \bar{\mathbf{D}}_L \mathbf{P}_1 \end{bmatrix}, \Delta = \begin{bmatrix} \mathbf{w}_1 \mathbf{D}_1 & \mathbf{w}_1 \mathbf{i} \\ \vdots & \vdots \\ \mathbf{w}_L \mathbf{D}_L & \mathbf{w}_L \mathbf{i} \end{bmatrix}. \quad (23)$$

The notations  $\bar{\mathbf{C}}_l$  and  $\bar{\mathbf{D}}_l$  are respectively defined as

$$\begin{aligned} \bar{\mathbf{C}}_l &= (\mathbf{A}_l^* \otimes \bar{\mathbf{A}}_l) [\text{vec}(\mathbf{e}_1 \mathbf{e}_1^T \mathbf{P}_1), \dots, \text{vec}(\mathbf{e}_K \mathbf{e}_K^T \mathbf{P}_1)] \\ &\quad + (\bar{\mathbf{A}}_l^* \otimes \mathbf{A}_l) [\text{vec}(\mathbf{P}_1 \mathbf{e}_1 \mathbf{e}_1^T), \dots, \text{vec}(\mathbf{P}_1 \mathbf{e}_K \mathbf{e}_K^T)], \\ \bar{\mathbf{D}}_l &= \mathbf{A}_l^* \odot \bar{\mathbf{A}}_l + \bar{\mathbf{A}}_l^* \odot \mathbf{A}_l, \end{aligned} \quad (24)$$

where

$$\bar{\mathbf{A}}_l = [\bar{\mathbf{a}}_{l,1}, \dots, \bar{\mathbf{a}}_{l,K}], \quad \bar{\mathbf{a}}_{l,k} = \frac{\partial \mathbf{a}_{l,k}}{\partial \theta_k}, \quad (25)$$

and  $\mathbf{e}_k \in \mathbb{R}^{K \times 1}$  contains one at the  $k$ -th position and zeros elsewhere.

*Proof:* The derivation can be found in Appendix A. ■

Compared with the general formula in (7) and the intermediate CRB expression in [43, Eq. 15] for two sources only, (19) is more compact and convenient for computing the CRBs

for multiple sources in different cases. Different from the CRB expression in [49, Eq. 2.24], which is valid only in the overdetermined case, (19) is applicable to both overdetermined and underdetermined cases, thereby suitable for assessing the performance of underdetermined wideband DOA estimation methods developed under the subband model, [36]–[38], [40], [46], [52], [54], [55].

#### IV. ANALYSES OF WIDEBAND STOCHASTIC CRBS

##### A. Relationship Between Wideband and Subband CRBs

It would be meaningful to compare the wideband underdetermined stochastic CRB with the narrowband one [45], [57], [67]. Such a comparison is valid in a statistical sense, because the CRB depends on the probability distribution of the data samples, regardless of which domain they belong to. Since the Fourier coefficients at each subband share a similar Gaussian distribution with the temporal samples in narrowband settings, we can apply the narrowband CRB expression to a single subband and study its relationship with the wideband CRBs.

*Corollary 1:* Consider the case with  $\mathcal{P}_u$ . Let  $\mathbf{B}(\boldsymbol{\theta}, l)$  denote the DOA-related block of the CRB for the  $l$ -th subband. Assume that the wideband and subband CRBs, i.e.,  $\mathbf{B}(\boldsymbol{\theta})$  and  $\{\mathbf{B}(\boldsymbol{\theta}, l)\}_{l=1}^L$ , all exist. Then,

$$\mathbf{B}^{-1}(\boldsymbol{\theta}) = \sum_{l=1}^L \mathbf{B}^{-1}(\boldsymbol{\theta}, l). \quad (26)$$

*Proof:* See Appendix B. ■

*Remark 2:* In fact, (26) reveals another relationship between the wideband and subband FIMs when  $\mathcal{P}_u$  is employed, i.e.,

$$\langle \tilde{\mathbf{F}}^{-1} \rangle_{\boldsymbol{\theta}}^{-1} = \sum_{l=1}^L \langle \mathbf{F}_l^{-1} \rangle_{\boldsymbol{\theta}}^{-1}, \quad (27)$$

where  $\langle \cdot \rangle_{\boldsymbol{\theta}}$  denotes the DOA-related block of the input argument. According to (4), a generic relationship is given by

$$\langle \tilde{\mathbf{F}}^{-1} \rangle_{\boldsymbol{\theta}}^{-1} = \left\langle \left( \sum_{l=1}^L \mathbf{F}_l \right)^{-1} \right\rangle_{\boldsymbol{\theta}}^{-1}. \quad (28)$$

Compared with (28), in (27), the summation operator is interchangeable with the inverse operator and  $\langle \cdot \rangle_{\boldsymbol{\theta}}$ , assuming all the subband FIMs are nonsingular. This implies the DOA parameters are decoupled with the nuisance parameters at each subband in the wideband FIM, so that the CRB for DOAs is independent of the nuisance blocks in the subband FIMs.

The relationship in *Corollary 1* provides an alternative formula for computing the wideband CRB with  $\mathcal{P}_u$ . It implies that in this case, the CRB for DOAs obtained by jointly processing all subbands of interest can be interpreted as a combination of those at each subband, if all the subband CRBs exist. However, this is true only if all the subband FIMs are nonsingular. It could happen that when the number of sources is relatively large, the FIM at each subband is singular, whereas the wideband FIM is nonsingular. This explains why more sources can be identified by processing multiple subbands, as advocated by most existing methods [36]–[38], [40], [41], [52].

In the other three cases with  $\mathcal{P}_f$ ,  $\mathcal{P}_{\text{up}}$ , and  $\mathcal{P}_{\text{uf}}$ , the relationship in *Corollary 1* does not hold, because the corresponding matrix  $\Delta$  is not block diagonal. Hence, when developing algorithms that employ any one of  $\mathcal{P}_f$ ,  $\mathcal{P}_{\text{up}}$ , and  $\mathcal{P}_{\text{uf}}$ , one should jointly process all subbands of interest.

### B. Order Relationship Among the Derived CRBs

In this subsection, we present the pairwise orders among the derived CRBs. For simplicity, we denote the CRB for DOAs in the four cases with  $\mathcal{P}_f$ ,  $\mathcal{P}_u$ ,  $\mathcal{P}_{up}$ , and  $\mathcal{P}_{uf}$  as  $\mathbf{B}_f$ ,  $\mathbf{B}_u$ ,  $\mathbf{B}_{up}$ , and  $\mathbf{B}_{uf}$ , respectively. The following lemma will be used.

*Lemma 1:* Employing the *a priori* knowledge that removes part of the nuisance parameters yields a lower CRB for DOAs.

*Proof:* See Appendix C. ■

By *Lemma 1*, the order relationship among the derived CRBs can be obtained as follows:

$$\mathbf{B}_{uf} \preceq \mathbf{B}_{up} \preceq \mathbf{B}_u, \quad \mathbf{B}_{uf} \preceq \mathbf{B}_f. \quad (29)$$

These inequalities indicate that using more available knowledge about the source spectra and the noise will improve the estimation accuracy. When developing DOA estimation methods aimed at special situations, one should utilize as much *a priori* knowledge as possible.

### C. Asymptotic Behavior with Respect to the Number of Snapshots

By (19), the CRB is inversely proportional to the number of frequency domain snapshots,  $Q$ , leading to

$$\lim_{Q \rightarrow \infty} \mathbf{B}_f = \lim_{Q \rightarrow \infty} \mathbf{B}_u = \lim_{Q \rightarrow \infty} \mathbf{B}_{up} = \lim_{Q \rightarrow \infty} \mathbf{B}_{uf} = 0. \quad (30)$$

Equation (30) illustrates the asymptotic behavior of the derived CRBs with respect to the number of snapshots under the condition that the duration of each subinterval  $\Delta t$  is constant. Given a fixed sampling frequency  $f_s$ , the duration of the observation interval  $Q\Delta t$  increases monotonically with the increase of the number of temporal snapshots  $N$ . To avoid an unbounded growth in the number of nuisance parameters,  $\Delta t$  should be constant [21]. On the other hand, for a fixed  $N$ , increasing  $Q$  causes decrease of  $\Delta t$ , which further broadens the bandwidth of each subband. This will reduce the number of effective subbands and in turn balance the influence imposed by the increase of  $Q$  on the CRB, which can be observed from (5). This agrees with the fact that once the observation interval is fixed, so is the amount of information contained in the data samples, even after these samples are transformed to the frequency domain.

### D. Asymptotic Behavior with Respect to SNR

We then investigate the asymptotic behavior of the wideband CRB with respect to SNR, especially in the case where  $\mathcal{P}_{uf}$  is employed. Notice that  $\mathcal{P}_{uf}$  comprises  $\mathcal{P}_f$  and  $\mathcal{P}_u$ , and it can be treated as a special case of  $\mathcal{P}_{up}$  with the proportional factors  $\{\xi_l\}_{l=2}^L$  being known. Thus, the asymptotic behavior of  $\mathbf{B}_{uf}$  can reflect that of  $\mathbf{B}_f$ ,  $\mathbf{B}_u$ , and  $\mathbf{B}_{up}$ .

Suppose that the sources are well separated, and the  $K$  sources have equal powers. By employing  $\mathcal{P}_{uf}$ , we assume  $\{\mathbf{P}_l\}_{l=1}^L = p\mathbf{I}_K$  with  $p \in \mathbb{R}_+$ . The noise power is also assumed to be identical across subbands, i.e.,  $\{\sigma_l\}_{l=1}^L = 1$ . Here,  $p$  represents not only the source power but also the SNR, which is sufficiently large.

*Theorem 2:* Consider the case where  $\mathcal{P}_{uf}$  is employed. Let  $\mathbf{B}_{uf}^{\text{asy}}$  denote the DOA-related block of the asymptotic wideband stochastic CRB for sufficiently large SNR. According to

the quantitative relationship between  $K$  and  $M$ ,  $\mathbf{B}_{uf}^{\text{asy}}$  takes the following different forms:

If  $M \leq K$ , then

$$\mathbf{B}_{uf}^{\text{asy}} = \frac{1}{Q} \left\{ \tilde{\mathbf{D}}^H \left[ \mathbf{\Gamma}_1 - \mathbf{\Gamma}_1 [\hat{\mathbf{D}}, \hat{\mathbf{i}}] \cdot \left( \begin{bmatrix} \hat{\mathbf{D}}^H \\ \hat{\mathbf{i}}^H \end{bmatrix} \mathbf{\Gamma}_1 [\hat{\mathbf{D}}, \hat{\mathbf{i}}] \right)^{-1} \begin{bmatrix} \hat{\mathbf{D}}^H \\ \hat{\mathbf{i}}^H \end{bmatrix} \mathbf{\Gamma}_1 \tilde{\mathbf{D}} \right] \right\}^{-1}. \quad (31)$$

If  $M > K$ , then

$$\mathbf{B}_{uf}^{\text{asy}} = \frac{1}{pQ} \left[ \tilde{\mathbf{D}}^H (\mathbf{\Gamma}_2 - L^{-1} \mathbf{\Gamma}_3 \mathbf{J} \mathbf{\Gamma}_3) \tilde{\mathbf{D}} \right]^{-1}. \quad (32)$$

The involved notations are defined as follows:

$$\begin{aligned} \tilde{\mathbf{D}} &= [\bar{\mathbf{D}}_1^T, \dots, \bar{\mathbf{D}}_L^T]^T, \quad \hat{\mathbf{D}} = [\mathbf{D}_1^T, \dots, \mathbf{D}_L^T]^T, \\ \mathbf{J} &= \mathbf{\Gamma}_4 \hat{\mathbf{D}} \hat{\mathbf{D}}^H \mathbf{\Gamma}_4 - (M - K)^{-1} \mathbf{\Gamma}_5 \hat{\mathbf{i}} \hat{\mathbf{i}}^H \mathbf{\Gamma}_5, \\ \hat{\mathbf{i}} &= \mathbf{1}_L \otimes \mathbf{i}, \end{aligned} \quad (33)$$

where  $\{\mathbf{\Gamma}_w\}_{w=1}^5$  denotes a group of block diagonal matrices (the definitions can be found in (D.6) and (D.11), Appendix D), and  $\mathbf{1}_L \in \mathbb{R}_+^{L \times 1}$  is an all-one vector.

*Proof:* See Appendix D. ■

From *Theorem 2*, we can see that in the overdetermined case, the asymptotic CRB decreases monotonically with the increase of SNR, and thus  $\lim_{p \rightarrow \infty} \mathbf{B}_{uf} = 0$ . In contrast, in the underdetermined case, the asymptotic CRB does not depend on the SNR. Hence, it can be inferred that the underdetermined wideband CRB will remain a finite, constant value when the SNR attains a certain threshold, hereafter, increasing the SNR brings limited performance gain. It is worth noting that *Theorem 2* provides theoretical explanations for the numerical results in [46], where  $\mathcal{P}_{uf}$  is studied.

### E. Rank Conditions for the Existence of the Derived CRBs

The previous derivation is based on the assumption that the wideband FIM is nonsingular. This condition can be interpreted as a specific rank condition on a certain matrix, which determines the existence of CRB [45], [67]. The rank conditions for the derived CRBs are shown below.

*Theorem 3:* Define the following matrices:

$$\begin{aligned} \Sigma_f &\triangleq \begin{bmatrix} \bar{\mathbf{C}}_1 & \mathbf{C}_1 \Psi & \mathbf{i} \\ \vdots & \vdots & \ddots \\ \bar{\mathbf{C}}_L & \mathbf{C}_L \Psi & \mathbf{i} \end{bmatrix}, \\ \Sigma_u &\triangleq \begin{bmatrix} \bar{\mathbf{D}}_1 \mathbf{P}_1 & \mathbf{D}_1 & & \mathbf{i} & & \\ \vdots & \ddots & & \ddots & & \\ \bar{\mathbf{D}}_L \mathbf{P}_L & & \mathbf{D}_L & & \mathbf{i} & \end{bmatrix}, \\ \Sigma_{up} &\triangleq \begin{bmatrix} \bar{\mathbf{D}}_1 \mathbf{P}_1 & \mathbf{D}_1 & \mathbf{0} & \cdots & \mathbf{0} & \mathbf{i} \\ \xi_2 \bar{\mathbf{D}}_2 \mathbf{P}_1 & \xi_2 \mathbf{D}_2 & \mathbf{D}_2 \mathbf{P}_1 & & & \mathbf{i} \\ \vdots & \vdots & & \ddots & & \vdots \\ \xi_L \bar{\mathbf{D}}_L \mathbf{P}_1 & \xi_L \mathbf{D}_L & & & \mathbf{D}_L \mathbf{P}_1 & \mathbf{i} \end{bmatrix}, \\ \Sigma_{uf} &\triangleq \begin{bmatrix} \bar{\mathbf{D}}_1 \mathbf{P}_1 & \mathbf{D}_1 & \mathbf{i} \\ \vdots & \vdots & \ddots \\ \bar{\mathbf{D}}_L \mathbf{P}_1 & \mathbf{D}_L & \mathbf{i} \end{bmatrix}. \end{aligned} \quad (34)$$

Then, the wideband stochastic CRBs, i.e.,  $\mathbf{B}_f$ ,  $\mathbf{B}_u$ ,  $\mathbf{B}_{up}$ , and  $\mathbf{B}_{uf}$  exist if and only if  $\Sigma_f$ ,  $\Sigma_u$ ,  $\Sigma_{up}$ , and  $\Sigma_{uf}$  have full column rank, respectively.

*Proof:* The rank condition for  $\Sigma_u$  has been proved in our earlier work, see *Theorem 1* in [1]. Since the four wideband CRBs share a common framework, the proofs of the other rank conditions can be carried out in a similar way. ■

## V. SOURCE RESOLVABILITY AND LINEAR ARRAYS

This section is devoted to a detailed study on source resolvability. We will show that the subband model itself can provide enhanced DOFs, which is the same goal achieved by the virtual co-array concept in most underdetermined methods. Based on a specific linear array, the subband model possesses superior resolvability and flexibility to the narrowband one. Furthermore, when certain *a priori* knowledge is available, the subband model shares similar features with the multi-frequency co-array augmentation concept and the non-coherent subarray system, both of which are effective solutions to the narrowband problem in the underdetermined case.

### A. Upper Bounds on Resolution Capacities

For the Gaussian distribution, nonsingularity of the FIM guarantees local identifiability of the unknown parameters [68]. Hence, the rank conditions in *Theorem 3* lead to several upper bounds on the resolution capacities (numbers of resolvable sources), which are shown below.

*Proposition 1:* Let  $K_f$ ,  $K_u$ ,  $K_{up}$ , and  $K_{uf}$  denote the resolution capacities based on an  $M$ -sensor array when  $\mathcal{P}_f$ ,  $\mathcal{P}_u$ ,  $\mathcal{P}_{up}$ , and  $\mathcal{P}_{uf}$  are employed, respectively. Then, the respective upper bounds on  $K_f$ ,  $K_u$ ,  $K_{up}$ , and  $K_{uf}$  are given by

$$\begin{aligned} K_f &\leq \sqrt{L(M^2 - 1)}, & K_u &\leq \frac{L}{L+1}(M^2 - 1), \\ K_{up} &\leq \frac{L}{2}(M^2 - 2) + \frac{1}{2}, & K_{uf} &\leq \frac{L}{2}(M^2 - 1). \end{aligned} \quad (35)$$

*Proof:* To guarantee that the matrices in (34) have full column rank, the number of columns in these matrices should be no larger than the number of rows, which yields a group of quadratic inequalities whose solutions are given by

$$\begin{aligned} K_f &\leq \sqrt{L(M^2 - 1) + \frac{1}{4}} - \frac{1}{2}, & K_u &\leq \frac{L}{L+1}(M^2 - 1), \\ K_{up} &\leq \frac{L}{2}(M^2 - 2) + \frac{1}{2}, & K_{uf} &\leq \frac{L}{2}(M^2 - 1). \end{aligned} \quad (36)$$

Notice that the involved variables are positive integers. In the first inequality,  $\sqrt{L(M^2 - 1) - 1} < \sqrt{L(M^2 - 1) + 1/4} - 1/2 < \sqrt{L(M^2 - 1)}$ , and thus  $K_f \leq \sqrt{L(M^2 - 1)}$ . The proof is complete. ■

From *Proposition 1*, we can see that the upper bounds on  $K_f$ ,  $K_{up}$ , and  $K_{uf}$  would be lifted with the increase of  $L$ . It appears that in these cases, one can resolve as many sources as possible with a sufficiently large  $L$ , which is not realistic. A large  $L$  will generate  $O(K^2L + L)$  nuisance parameters in the general subband model, possibly resulting in overparameterization that arises before  $\mathcal{P}_f$  reduces the number of nuisance parameters. When this happens, the wideband FIM might be very close to singular, and the CRB should be calculated by the Moore–Penrose pseudo inverse of the FIM [69]. The price paid for model order mismatch is a large

estimation variance. Therefore, it is not always desirable to process all subbands, as mentioned in Section II. In fact, the nature of the physical array imposes an effective resolution capacity, which is only improved by an additive factor of  $o(\ln L)$  beyond  $M - 1$  as  $L$  increases [49].

On the other hand,  $K_u$  is primarily restricted to  $M^2 - 1$ . This indicates that up to  $O(M^2)$  sources can be resolved by an  $M$ -sensor array, which coincides with the number of DOFs provided by typical sparse arrays, see, e.g., [25]. This means that the subband model itself plays a role as important as sparse arrays in underdetermined DOA estimation, and we shall discuss this property in detail in Section V-B.

The upper bounds in (35) are, in general, ideal. However, they still offer valuable guidance on developing underdetermined techniques. To improve the resolvability of spatially uncorrelated sources, one should use more physical sensors rather than processing more subbands. On the other hand, when the source spectra is known to be flat or proportional, one could exploit more subbands to reach the effective resolution capacity while reducing hardware complexity or dealing with physical size constraints.

### B. Possibility for Underdetermined DOA Estimation Based on Linear Arrays

The results above apply to various array geometries as long as there is only one unknown angular parameter for each source. In this subsection, we focus on linear arrays and explore the possibility for underdetermined DOA estimation in different cases. Starting from the case with  $\mathcal{P}_u$ , a concise review of the difference co-array concept is first presented.

Consider a linear array consisting of  $M$  sensors and let  $d$  denote the unit inter-sensor spacing. The position of the  $m$ -th sensor can be expressed as  $z_m d$ ,  $z_m \in \mathbb{R}$ . Then, the array structure can be represented by a real set  $\mathbb{A} = \{z_1, \dots, z_M\}$ . Introduce the difference set such that

$$\mathbb{A}_{\text{diff}} = \{z_{m_1} - z_{m_2} \mid z_{m_1}, z_{m_2} \in \mathbb{A}; m_1, m_2 = 1, \dots, M\}. \quad (37)$$

Let  $\mathbb{D}$  collect all unique elements of  $\mathbb{A}_{\text{diff}}$  in ascending order, and then  $\mathbb{D}$  represents the corresponding difference co-array.

For the  $l$ -th subband, the  $(m, k)$ -th element of the array manifold matrix for the linear array  $\mathbb{A}$  can be written as

$$\langle \mathbf{A}_l \rangle_{m,k} = e^{-j2\pi \frac{d}{\lambda_l} z_m \sin \theta_k}, \quad (38)$$

where  $\lambda_l = c/f_l$  with  $c$  representing the wave speed, and  $j = \sqrt{-1}$  is the imaginary unit. Substituting (38) into (14), we can write the  $(\bar{m}, k)$ -th element of  $\mathbf{D}_l$  as

$$\begin{aligned} \langle \mathbf{D}_l \rangle_{\bar{m},k} &= e^{-j2\pi \frac{d}{\lambda_l} (z_{m_1} - z_{m_2}) \sin \theta_k}, \\ \bar{m} &= (m_2 - 1)M + m_1. \end{aligned} \quad (39)$$

Clearly,  $\mathbf{D}_l$  is associated with  $\mathbb{A}_{\text{diff}}$ , and the number of unique rows in  $\mathbf{D}_l$  equals  $|\mathbb{D}|$ , i.e., the number of DOFs.

The possibility for resolving more wideband Gaussian sources than the number of physical sensors is shown below.

*Proposition 2:* Based on a linear array consisting of  $M$  sensors, it is possible to resolve the following numbers of sources when  $\mathcal{P}_f$ ,  $\mathcal{P}_u$ ,  $\mathcal{P}_{up}$ , and  $\mathcal{P}_{uf}$  are employed, respectively.

$$K_f \geq M, K_u > \frac{|\mathbb{D}|-1}{2}, K_{up} \geq |\mathbb{D}| > M, K_{uf} \geq |\mathbb{D}| > M. \quad (40)$$

Compared to the upper bound on  $K_u$  in (36), a tighter bound is given by

$$K_u \leq \frac{L}{L+1}(|\mathbb{D}| - 1). \quad (41)$$

*Proof:* See Appendix E. ■

For a uniform linear array (ULA) whose first sensor is located at  $0d$ , we have  $|\mathbb{D}| = 2M - 1$ . Then, the resolution capacity with  $\mathcal{P}_u$  satisfies  $M - 1 < K_u < 2M - 1$ , violating the overdetermined limitation. The upper bound in (41) is a special case for linear arrays, and it is always tighter than the general one in (35), because  $|\mathbb{D}| < M^2, \forall M > 1$ . Thus, when a linear array is employed, the resolution capacity employing  $\mathcal{P}_u$  is essentially determined by the number of DOFs provided by the difference co-array.

To conduct underdetermined DOA estimation for narrowband signals, a sparse array is indispensable, because the number of resolvable narrowband sources (known *a priori* to be spatially uncorrelated), denoted by  $K_u^{\text{narrow}}$ , is upper bounded by  $K_u^{\text{narrow}} \leq (|\mathbb{D}| - 1)/2$  [45], [67], which becomes  $K_u^{\text{narrow}} \leq M - 1$  for a ULA. In contrast, underdetermined DOA estimation for wideband signals is feasible as long as certain *a priori* knowledge about the source spectra is employed, whereas a sparse linear array is not needed, as shown in (40). Moreover, more wideband Gaussian sources than narrowband ones can be resolved based on a given linear array, either uniform or sparse.

Furthermore, (40) implies that resolving more wideband Gaussian sources than the number of DOFs provided by the difference co-array is possible with the assistance of  $\mathcal{P}_{up}$  or  $\mathcal{P}_{uf}$ . This property will be verified later in Section VI.

### C. Further Interpretation of the Subband Model

In this subsection, we seek to find the connection between the subband model and other scenarios that are also suitable for underdetermined DOA estimation in the narrowband case.

Choose a reference frequency  $f_0$  and denote the corresponding wavelength as  $\lambda_0 = c/f_0$ . Then,  $\lambda_l$  can be expressed as  $\lambda_l = \nu_l \lambda_0$  with  $\nu_l \in \mathbb{R}_+$  being a positive coefficient. We can rewrite (38) as

$$\langle \mathbf{A}_l \rangle_{m,k} = e^{-j2\pi \frac{d}{\lambda_0} \bar{z}_{l,m} \sin \theta_k}, \quad (42)$$

where  $\bar{z}_{l,m} = z_m/\nu_l$ . Hence,  $\mathbf{A}_l$  is equivalent to the array manifold matrix of a scaled array operating at  $f_0$ , whose sensor positions are given by  $\bar{\Delta}_l = \{\bar{z}_{l,1}, \dots, \bar{z}_{l,M}\}$  in unit of  $d$ .

As such,  $\mathbf{X}_{l,q}$  in (2) can be treated as the measurement of the  $l$ -th scaled array output in the spatio-frequency domain. In (2),  $\mathbf{S}_{l,q}$  varies with  $l$ , and consequently,  $\{\mathbf{X}_{l,q}\}_{l=1}^L$  cannot be regarded as the output signal of an augmented virtual array consisting of all scaled subarrays. This feature makes the signal representation under the subband model differ from that under the narrowband co-array model [25]–[28], where

the signal waveforms received by all the sensors are identical. Alternatively, (2) can be interpreted as follows.

There exist  $L$  subarrays receiving frequency domain signals emitted by  $K$  narrowband sources, corrupted by additive Gaussian white noise. All subarrays consist of  $M$  sensors, but with distinct sensor positions. The source spectra and the noise spectra vary from one subarray to another, and the signal waveforms received at different subarrays are uncorrelated. Moreover, when different *a priori* knowledge is employed, the corresponding interpretations are given as follows.

- With  $\mathcal{P}_f$ , the auto-covariance matrices of the source signals are known *a priori* to be identical across subarrays.
- With  $\mathcal{P}_u$ , the sources are known *a priori* to be spatially uncorrelated.
- With  $\mathcal{P}_{up}$ , the sources are known *a priori* to be spatially uncorrelated and have proportional powers across subarrays.
- With  $\mathcal{P}_{uf}$ , the sources are known *a priori* to be spatially uncorrelated and have identical powers across subarrays.

With  $\mathcal{P}_{up}$ , the interpreted model shares the same settings as the multi-frequency co-array augmentation concept [54], where the frequency diversity of uncorrelated sources with proportional powers can generate different virtual subarrays to fill the holes in the augmented difference co-array, thus offering enhanced DOFs based on a physical ULA. With  $\mathcal{P}_f$ , the interpreted model is a special case of the non-coherent subarray system, where the number of sensors in all subarrays are identical. Recently, it has been shown that this system can resolve more sources than those by each subarray [70].

These close connections imply that the wideband CRB framework in (19) can be used to compute the CRBs in the two aforementioned scenarios. Conversely, the optimization schemes in these two scenarios, such as the frequency selection strategies for multi-frequency sources and the subarray design techniques for the non-coherent subarray system, can be extended to the wideband scenario to improve source resolvability and estimation accuracy. An example that invokes this idea can be found in our previous paper [39] and a very recent one [42], where a novel design for the inter-sensor spacing of a physical ULA and the corresponding group-sparsity based method are proposed, which can resolve many more linear frequency modulated continuous waveform signals than the number of sensors in the ULA.

## VI. SIMULATIONS

In this section, simulations are conducted using the Multiprecision Computing Toolbox for MATLAB with a default precision of 34 decimal digits. Throughout this section, we set the sources to be spatially uncorrelated with flat spectra; however, not all the information is known *a priori*. The  $K$  sources are uniformly located in  $[-60^\circ, 60^\circ]$  with equal powers at each subband. The number of DFT points is  $L_0 = 64$ . The central frequency of the  $l$ -th subband is  $f_l = (l - 1)f_s/L_0$ . The unit inter-sensor spacing is  $d = c/f_s$ . The following linear array structures will be used, including a 7-sensor ULA, a 10-sensor

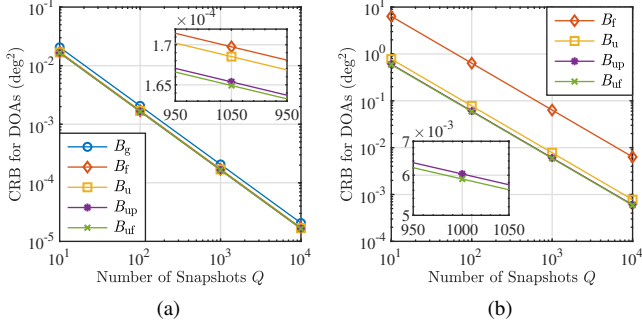


Fig. 1. Wideband CRBs versus the number of snapshots (a) in the overdetermined case, and (b) in the underdetermined case.

ULA, a (2,3) co-prime array [26], and a (3,3) two-level nested array [25]. Their sensor positions are respectively denoted by

$$\begin{aligned} \mathbb{A}_{\text{ULA}(7)} &= \{0, 1, 2, 3, 4, 5, 6\}, \\ \mathbb{A}_{\text{ULA}(10)} &= \{0, 1, 2, 3, 4, 5, 6, 7, 8, 9\}, \\ \mathbb{A}_{\text{co-prime}(2,3)} &= \{0, 2, 3, 4, 6, 9\}, \\ \mathbb{A}_{\text{nested}(3,3)} &= \{1, 2, 3, 4, 8, 12\}. \end{aligned} \quad (43)$$

In each experiment, the averaged CRB for all DOAs is recorded.

#### A. Wideband CRBs versus the Number of Snapshots

In the first set of simulations, we investigate the four derived wideband CRBs, i.e.,  $\mathbf{B}_f$ ,  $\mathbf{B}_u$ ,  $\mathbf{B}_{up}$ , and  $\mathbf{B}_{uf}$ , versus the number of snapshots  $Q$ . For comparison, the wideband CRB for the general case without *a priori* knowledge [49], denoted by  $\mathbf{B}_g$ , is also considered. We use the nested array  $\mathbb{A}_{\text{nested}(3,3)}$  with  $M = 6$  and set SNR = 10 dB. There are  $L = 16$  subbands of interest in total with indexes from 17 to 32.

We set  $K = 5$  and  $K = 10$  for the overdetermined case and the underdetermined case, respectively. The CRB results are shown in Fig. 1. It can be observed from Fig. 1(a) and Fig. 1(b) that all the CRB curves are inversely proportional to the number of snapshots. In the overdetermined case,  $\mathbf{B}_g$  is the largest, while the curves of  $\mathbf{B}_f$ ,  $\mathbf{B}_u$ ,  $\mathbf{B}_{up}$ , and  $\mathbf{B}_{uf}$  stay very close to each other. In the underdetermined case,  $\mathbf{B}_g$  is excluded since it becomes invalid, and the differences among  $\mathbf{B}_f$ ,  $\mathbf{B}_u$ ,  $\mathbf{B}_{up}$ , and  $\mathbf{B}_{uf}$  become more noticeable. Through the relative positions of the CRB curves, the order relationship in (29) can be clearly verified in either Fig. 1(a) or Fig. 1(b).

#### B. Wideband CRBs versus SNR

The second set of simulations examines the four derived CRBs versus SNR with the number of snapshots  $Q = 500$ . We use the ULA  $\mathbb{A}_{\text{ULA}(10)}$  with  $M = 10$  and consider  $L = 16$  subbands whose indexes cover from 17 to 32.

In the overdetermined case, we set the number of sources as  $K = 8$ . Fig. 2(a) shows that all the five CRB curves decrease monotonically with the increase of SNR, and they show strong inverse logarithmic dependence on the SNR when it exceeds 0 dB. When the SNR is lower than 0 dB, the distances among the five CRBs are visibly larger, implying that the potential

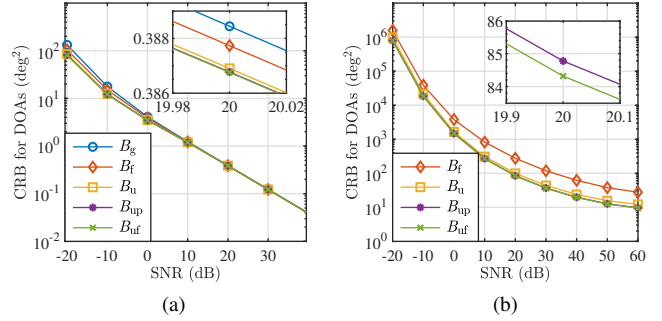


Fig. 2. Wideband CRBs versus SNR (a) in the overdetermined case, and (b) in the underdetermined case.

performance gain brought by employing *a priori* knowledge is more significant only in the low-SNR region. Moreover, the four CRBs with different *a priori* knowledge are always lower than the general one, and their differences are hardly noticeable in the whole SNR region, which means that only one type of *a priori* knowledge is enough to bring satisfactory performance gain. These observations coincide and extend the numerical results in [43] for the dual-source case.

In the underdetermined case, we set  $K = 12$ . Fig. 2(b) shows that the dependence of the four CRB curves on the SNR becomes more and more negligible as SNR increases. Note that the four CRBs exist in the underdetermined case even if a ULA is employed here. Moreover, there is little difference among  $\mathbf{B}_u$ ,  $\mathbf{B}_{up}$ , and  $\mathbf{B}_{uf}$  in the whole SNR region, whereas the distance from  $\mathbf{B}_f$  to the other three is more significant. This means that employing  $\mathcal{P}_u$  brings more performance gain than  $\mathcal{P}_f$ . In addition, the order relationship in (29) can also be verified in either Fig. 2(a) or Fig. 2(b).

#### C. Relationship Between Wideband and Subband CRBs

The third set of simulations examines the relationship between the wideband CRB and the subband ones, as presented in *Corollary 1*.  $L = 16$  subbands are considered with indexes from 17 to 32. The number of snapshots is  $Q = 500$ .

In the overdetermined case, we adopt the ULA  $\mathbb{A}_{\text{ULA}(10)}$  with  $M = 10$  and set  $K = 2, 9$ . In the underdetermined case, we use the co-prime array  $\mathbb{A}_{\text{co-prime}(2,3)}$  with  $M = 6$  and set  $K = 8, 10$ . In Fig. 3, the CRB results computed from the left-hand side and right-hand side of (26) are denoted by  $\mathbf{B}_u^{\text{wide}}$  and  $\mathbf{B}_u^{\text{sub}}$ , respectively. It can be observed that both results are consistent, which verifies *Corollary 1*.

#### D. Asymptotic CRB Expressions for Sufficiently Large SNR

In the fourth set of simulations, we examine the asymptotic CRB expressions proposed in *Theorem 2*. The co-prime array  $\mathbb{A}_{\text{co-prime}(2,3)}$  is used with  $M = 6$  and  $Q = 500$ .  $L = 16$  subbands are of interest with indexes from 17 to 32.

In the overdetermined case, set  $K = 1, 5$ . Fig. 4(a) shows that  $\mathbf{B}_{uf}^{\text{asy}}$  is inversely logarithmic proportional to the SNR. In the underdetermined case, set  $K = 6, 7$ . Fig. 4(b) shows that  $\mathbf{B}_{uf}^{\text{asy}}$  is a positive constant, independent from the SNR. Obviously, the true CRB values (solid lines) indeed converge

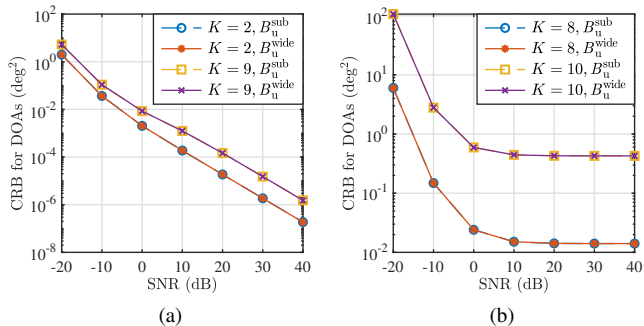


Fig. 3. Results for the wideband CRB employing  $\mathcal{P}_u$  computed from both sides of Eq. (26), (a) in the overdetermined case, and (b) in the underdetermined case.

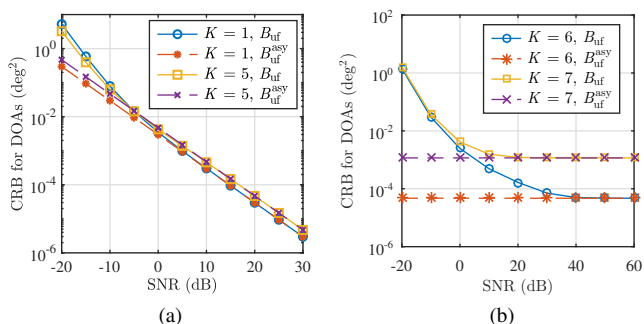


Fig. 4. Asymptotic CRBs for sufficiently large SNR (a) in the overdetermined case, and (b) in the underdetermined case.

to the asymptotic ones (dashed lines) when the SNR exceeds 20 dB in Fig. 4(a) and 40 dB in Fig. 4(b), respectively.

### E. Wideband CRBs versus the Number of Sources

In the fifth simulation,  $B_f$ ,  $B_u$ ,  $B_{up}$ , and  $B_{uf}$  are examined versus a varying number of sources  $K$ , with  $Q = 500$  and SNR = 10 dB. We use  $L = 63$  subbands whose indexes cover from 2 to 64. For comparison, we also include the wideband CRB for the general case,  $B_g$ , and apply the narrowband CRB with  $\mathcal{P}_u$  [57], [67] to the 56th subband, denoted by  $B_{56th\_sub}$ . As stated in Section IV-A, such a comparison is valid in a statistical sense, and the existence of wideband and subband CRBs will show the difference between the resolution capacities in the wideband and narrowband scenarios. We use the co-prime array  $\mathbb{A}_{co\text{-}prime(2,3)}$  with  $M = 6$ , and the corresponding difference co-array is  $\mathbb{D}_{co\text{-}prime(2,3)} = \{-9, -7, \dots, 7, 9\}$  with the number of DOFs  $|\mathbb{D}_{co\text{-}prime(2,3)}| = 17$ .

In general, as  $K$  increases, the FIM tends to be singular, and the CRB grows larger. If  $K$  reaches the value where the FIM turns out to be singular, a breakpoint (or a divergent point towards infinity) will occur in the CRB curve. The value of  $K$  associated with the breakpoint links to the resolution capacity, i.e.,  $K - 1$ . The breakpoints of the curves in Fig. 5 indicate that the ranges where  $B_g$ ,  $B_f$ ,  $B_u$ ,  $B_{up}$ , and  $B_{uf}$  exist are  $1 \leq K_g \leq 5$ ,  $1 \leq K_f \leq 18$ ,  $1 \leq K_u \leq 14$ ,  $1 \leq K_{up} \leq 23$ , and  $1 \leq K_{uf} \leq 23$ , respectively. These results coincide with the inequalities proposed in (35), (40), and (41). Except for

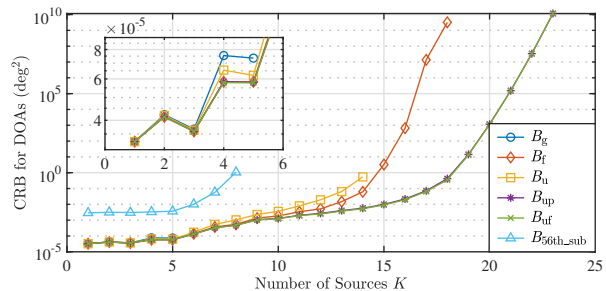


Fig. 5. Wideband CRBs and the CRB for the 56th subband versus the number of sources.

$B_g$ , all the other CRBs exist when  $K \geq 6$ , which implies the existence of unbiased underdetermined DOA estimators in the corresponding cases. In particular,  $K_{up}$  and  $K_{uf}$  can be larger than  $|\mathbb{D}_{co\text{-}prime(2,3)}|$ , implying that the number of resolvable wideband sources can even exceed the number of DOFs provided by the difference co-array.

When  $K > 8$ , the subband CRB  $B_{56th\_sub}$  becomes invalid, which is consistent with the resolution capacity for uncorrelated narrowband sources, i.e.,  $K_{u}^{narrow} \leq (|\mathbb{D}_{co\text{-}prime(2,3)}| - 1)/2$ . In contrast, the wideband FIMs with different *a priori* knowledge remain nonsingular as  $K$  increases. This indicates that more wideband Gaussian sources can be resolved than the narrowband ones based on the same array.

Moreover, a part of the subband FIMs becomes singular when  $K > 8$ , so that the wideband FIM tends to be singular as  $K$  increases, leading to sharp growth of the CRB values. We can see from the curves of  $B_f$ ,  $B_{up}$ , and  $B_{uf}$  that the CRBs will be significantly large when  $K$  exceeds certain values. This means that achieving superior resolvability will greatly sacrifice the estimation accuracy. According to the asymptotic behavior of the CRBs with respect to  $Q$ , a sufficiently large number of snapshots of the same quantity level should be exploited to mitigate the loss of estimation accuracy. Intriguingly,  $B_{up}$  and  $B_{uf}$  almost coincide, meaning that employing  $\mathcal{P}_{up}$  or  $\mathcal{P}_{uf}$  brings almost the same performance improvement. In addition, the effective resolution capacity can be approximately determined by specifying  $K$  when the CRB exceeds a certain value.

### F. Performance Analyses Using the Derived CRBs

The sixth set of simulations is aimed at illustrating the practical value of derived CRBs. We shall evaluate the performance of some existing wideband DOA estimation methods developed for the underdetermined case, such as the SS-MUSIC [36], the SS-CSSM [71] (the conventional CSSM followed by a SS process), and the CS-based method [41], all of them employ  $\mathcal{P}_u$ . Since the CRB values and the resolution capacities with  $\mathcal{P}_{up}$  and  $\mathcal{P}_{uf}$  are almost the same, (as shown in Figs. 1, 2, and 5), we shall focus on a modified CS-based method employing  $\mathcal{P}_{uf}$ . At present, it seems immature to analyze the performance of underdetermined DOA estimation methods employing  $\mathcal{P}_f$  only, because such methods have not been reported, to the best of our knowledge. In what follows, DOA estimation is performed based on a search grid from

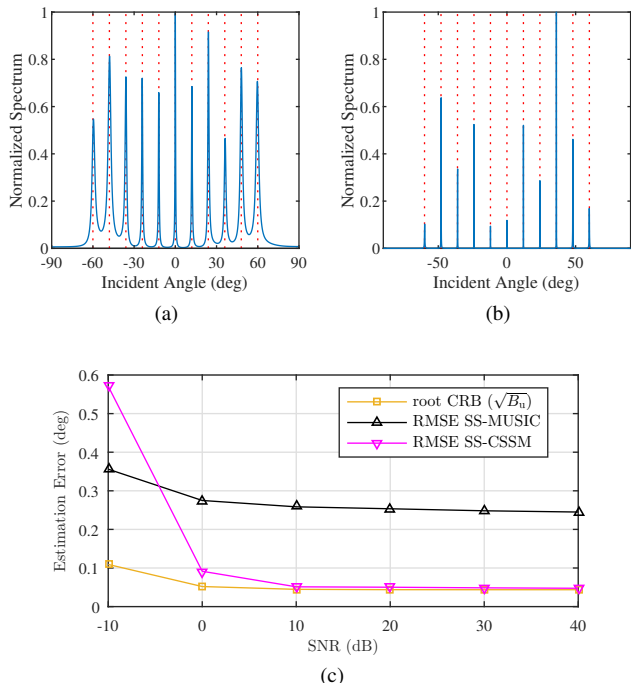


Fig. 6. DOA estimation results using two SS-based methods. (a) Estimated normalized spectrum by the SS-MUSIC. (b) Estimated normalized spectrum by the SS-CSSM. (c) RMSEs and root CRB versus SNR.

$-90^\circ$  to  $90^\circ$  with a step size of  $0.1^\circ$ , and  $Q = 500$ . The root mean squared errors (RMSEs) of all the algorithms considered are obtained through 200 Monte Carlo trials.

First, we adopt the nested array  $\mathbb{A}_{\text{nested}(3,3)}$  with  $M = 6$  and  $K = 11$ .  $L = 63$  subbands are of interest with indexes from 2 to 64. DOA estimation results of the SS-MUSIC and the SS-CSSM with SNR = 10 dB are presented in Figs. 6(a) and (b), respectively, where the blue lines represent the estimated normalized spectrum, and the red dashed lines are the true DOAs. We can see that all the 11 sources are correctly resolved by both methods. The RMSEs and the root CRB are plotted in Fig. 6(c) with respect to SNR. The CRB curve is always lower than the two RMSE curves, which means that  $B_u$  indeed provides an appropriate performance benchmark for the two SS-based methods. It is shown that the performance of the SS-CSSM is near optimal when the SNR exceeds 10 dB, whereas it degenerates rapidly in the low SNR region. In contrast, the SS-MUSIC performs better when the SNR is low, while its performance in the high-SNR region can be improved.

We then use the ULA  $\mathbb{A}_{\text{ULA}(7)}$  with  $M = 7$  and  $K = 9$ .  $L = 17$  subbands whose indexes cover from 48 to 64 are of interest. The CS-based method [41] is employed, and the results with SNR = 10 dB is plotted in Fig. 7(a). Clearly, all the 9 sources are successfully identified by the method, indicating that it is feasible to perform underdetermined DOA estimation for wideband sources based on a ULA. The RMSE and root CRB versus SNR are presented in Fig. 7(b), showing that  $B_u$  is a suitable performance bound for the CS-based method. In addition, the estimation accuracy of the CS-based method is not far from optimal.

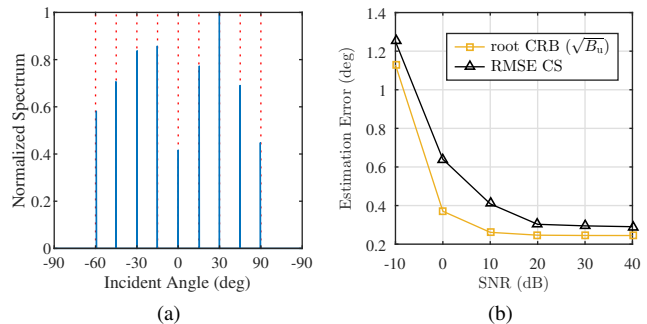


Fig. 7. DOA estimation results using the CS-based method. (a) Estimated normalized spectrum. (b) RMSE and root CRB versus SNR.

Finally, we propose a modified CS-based method utilizing  $\mathcal{P}_{\text{uf}}$ . The modification is carried out as follows. The CS-based method combines the equivalent signal representations in (13) at all subbands of interest, and then formulates a convex optimization problem based on the group sparsity concept. In the original formulation [41, Eq. 23], the equivalent steering matrices  $\{D_l\}_{l=1}^L$  are collected by a block diagonal matrix, and the unknown parameters in the source spectra  $\{p_l\}_{l=1}^L$  are held by a column vector. Incorporating the effect of  $\mathcal{P}_f$ ,  $\{D_l\}_{l=1}^L$  should be concatenated following the column direction, and  $\{p_l\}_{l=1}^L$  turn out to be independent of  $l$ . Therefore, the difference co-arrays at all subbands of interest jointly behave as an augmented virtual array, and the new formulation fits the narrowband convex optimization problem [41, Eq. 10].

We use the co-prime array  $\mathbb{A}_{\text{co-prime}(2,3)}$  with  $M = 6$  and  $K = 18$ .  $L = 63$  subbands are of interest with indexes from 2 to 64. As predicted by Fig. 5, the original CS-based method employing  $\mathcal{P}_u$  cannot resolve all the 18 sources, whereas the modified one employing  $\mathcal{P}_{\text{uf}}$  can. The DOA estimation results using the original method with SNR = 10 dB is presented in Fig 8(a), where several false peaks occur and not all the 18 sources can be resolved. On the other hand, Fig 8(b) shows the results produced by the modified method with SNR = 10 dB, where all the sources are correctly identified, indicating that resolving more sources than the number of DOFs offered by the difference co-array is indeed feasible by employing  $\mathcal{P}_{\text{uf}}$ . Furthermore, the RMSE of the modified method and the root CRB are presented in Fig. 8(c), showing that  $B_{\text{uf}}$  offers a proper performance bound for the modified CS-based method. Although the modified method has strong source resolvability, its estimation accuracy can still be improved.

## VII. CONCLUSION

In this paper, the wideband stochastic CRBs with different *a priori* knowledge have been studied under the subband model via frequency decomposition. A unified CRB framework for the DOA related-blocks has been derived, which encompasses a class of closed-form expressions when four types of popular *a priori* knowledge are employed, respectively. These CRB expressions are applicable to the underdetermined case where existing wideband CRB results become invalid, providing performance assessment tools for existing and future underdetermined wideband DOA estimation algorithms.

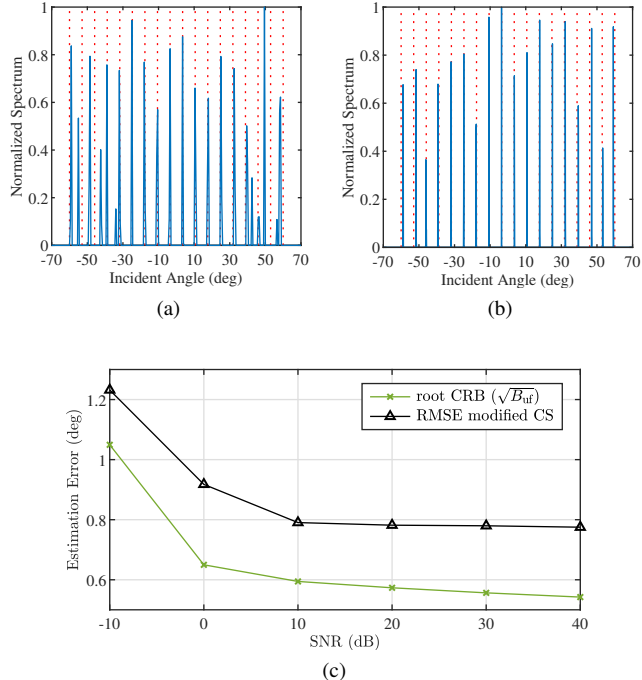


Fig. 8. DOA estimation results using two CS-based methods. (a) Estimated normalized spectrum by the original CS-based method employing  $\mathcal{P}_u$ . (b) Estimated normalized spectrum by the modified CS-based method employing  $\mathcal{P}_{uf}$ . (c) RMSE of the modified CS-based method and root CRB versus SNR.

The relationship between the wideband CRB and the subband ones were investigated. Particularly, in the case with  $\mathcal{P}_u$ , the wideband CRB can be interpreted by the subband ones. Through order comparison among the derived CRBs, it was proved that more *a priori* knowledge will reduce the CRB for DOAs. Their asymptotic behavior with respect to the number of snapshots and SNR has been examined, with two asymptotic expressions derived for sufficiently large SNR. With the increase of SNR, the CRB approaches to zero in the overdetermined case, while it converges to a positive constant in the underdetermined case, indicating that increasing the input SNR would not bring much performance gain for underdetermined DOA estimation.

Existence of the derived CRBs was examined through rank conditions of the introduced matrices, yielding several upper bounds on resolution capacities. As discussed, the subband model itself can offer enhanced DOFs to achieve underdetermined estimation without the aid of sparse arrays. Based on a given linear array (uniform or sparse), one can resolve more wideband Gaussian sources than narrowband ones. By employing  $\mathcal{P}_{up}$  or  $\mathcal{P}_{uf}$ , the number of resolvable wideband sources can even exceed the number of DOFs offered by the difference co-array. Further interpretations of the subband model established the underlying connections with the multi-frequency co-array augmentation concept and the non-coherent subarray system, implying potential extensions of optimization techniques among these scenarios.

## APPENDIX A PROOF OF THEOREM 1

First, we calculate  $\partial r_l / \partial \alpha^T$  in different cases.

If  $\mathcal{P}_f$  is employed, (10) and (15) should be used, yielding

$$\frac{\partial r_l}{\partial \alpha^T} = [\bar{\mathbf{C}}_l \mathbf{P}_l, \mathbf{C}_l \boldsymbol{\Psi}, \mathbf{f}_l \otimes \mathbf{i}], \quad (\text{A.1})$$

where  $\mathbf{f}_l \in \mathbb{R}^{1 \times L}$  contains one at the  $l$ -th position and zeros elsewhere.

If  $\mathcal{P}_u$  is employed, (13) and (16) should be used, yielding

$$\frac{\partial r_l}{\partial \alpha^T} = [\bar{\mathbf{D}}_l \mathbf{P}_l, \mathbf{f}_l \otimes \mathbf{D}_l, \mathbf{f}_l \otimes \mathbf{i}]. \quad (\text{A.2})$$

If  $\mathcal{P}_{up}$  is employed, (13) and (17) should be used, yielding

$$\frac{\partial r_l}{\partial \alpha^T} = \begin{cases} [\bar{\mathbf{D}}_1 \mathbf{P}_1, \mathbf{D}_1, \mathbf{0}_{M^2 \times (L-1)}, \mathbf{f}_1 \otimes \mathbf{i}], & l = 1. \\ [\xi_l \bar{\mathbf{D}}_l \mathbf{P}_l, \xi_l \mathbf{D}_l, \mathbf{f}_l \otimes (\mathbf{D}_l \mathbf{P}_1), \mathbf{f}_l \otimes \mathbf{i}], & l = 2, \dots, L. \end{cases} \quad (\text{A.3})$$

If  $\mathcal{P}_{uf}$  is employed, (13) and (18) should be used, yielding

$$\frac{\partial r_l}{\partial \alpha^T} = [\bar{\mathbf{D}}_l \mathbf{P}_l, \mathbf{D}_l, \mathbf{f}_l \otimes \mathbf{i}]. \quad (\text{A.4})$$

Substituting (A.1), (A.2), (A.3), and (A.4), respectively, into (7) yields the inverse of four CRB matrices which all fit into the following framework:

$$\mathbf{B}^{-1}(\boldsymbol{\alpha}) = \mathbf{Q} \begin{bmatrix} \mathbf{G}^H \\ \boldsymbol{\Delta}^H \end{bmatrix} [\mathbf{G}, \boldsymbol{\Delta}]. \quad (\text{A.5})$$

Explicit expressions of  $\mathbf{G}$  and  $\boldsymbol{\Delta}$  can be found in (20), (21), (22), and (23). Then, using the standard result on the inversion of a partitioned matrix [58, Section A.7], we can obtain (19), which completes the proof.

## APPENDIX B PROOF OF COROLLARY 1

By (21),  $\boldsymbol{\Delta}$  is block diagonal, so that the orthogonal projector  $\boldsymbol{\Pi}_{\boldsymbol{\Delta}}^\perp$  is also block diagonal. As a result, (19) can be rewritten as

$$\mathbf{B}(\boldsymbol{\theta}) = \left( \mathbf{Q} \sum_{l=1}^L \mathbf{G}_l^H \boldsymbol{\Pi}_{\boldsymbol{\Delta}}^\perp \mathbf{G}_l \right)^{-1}, \quad (\text{B.1})$$

where

$$\mathbf{G}_l = \mathbf{W}_l \bar{\mathbf{D}}_l \mathbf{P}_l, \quad \boldsymbol{\Delta}_l = [\mathbf{W}_l \mathbf{D}_l, \mathbf{W}_l \mathbf{i}]. \quad (\text{B.2})$$

Applying the narrowband stochastic CRB employing  $\mathcal{P}_u$  [57] to the  $l$ -th subband leads to

$$\mathbf{B}(\boldsymbol{\theta}, l) = (\mathbf{Q} \mathbf{G}_l^H \boldsymbol{\Pi}_{\boldsymbol{\Delta}}^\perp \mathbf{G}_l)^{-1}. \quad (\text{B.3})$$

Substituting (B.3) into (26) and taking the inverse yields (B.1), which completes the proof.

## APPENDIX C PROOF OF COROLLARY 2

We introduce the following lemma [3] to carry out the proof.

*Lemma 2:* Consider a positive definite matrix  $\mathcal{A} \in \mathbb{C}^{u \times u}$  partitioned as  $\mathcal{A} = \begin{bmatrix} \mathcal{A}_1 & \mathcal{A}_2 \\ \mathcal{A}_2^H & \mathcal{A}_3 \end{bmatrix}$ , where  $\mathcal{A}_1 \in \mathbb{C}^{v \times v}$ . Let  $\mathcal{S} \in \mathbb{C}^{u \times w}$  be another partitioned matrix such that  $\mathcal{S} = [\mathcal{S}_1^T, \mathcal{S}_2^T]^T$  with  $\mathcal{S}_1 \in \mathbb{C}^{v \times w}$ . Then,  $\mathcal{S}_1^H \mathcal{A}_1^{-1} \mathcal{S}_1 \preceq \mathcal{S}^H \mathcal{A}^{-1} \mathcal{S}$ . The equality holds if and only if  $\mathcal{A}_2^H \mathcal{A}^{-1} \mathcal{S}_1 = \mathcal{S}_2$ .

Let  $\epsilon_0$  denote the nuisance parameter vector in the original parametric model. Employing *a priori* knowledge will remove part of the nuisance parameters collected by  $\epsilon_2$ , while the left ones are held by  $\epsilon_1$ . Introduce the notation  $\Delta_\beta = \partial \mathbf{r}_l / \epsilon_\beta^T$ ,  $\beta = 0, 1, 2$ , and then we can write

$$\Delta_0 \Omega = [\Delta_1, \Delta_2], \quad (\text{C.1})$$

where  $\Omega$  is a permutation matrix satisfying [72]

$$\Omega^{-1} = \Omega^T. \quad (\text{C.2})$$

Since *a priori* knowledge does not affect the DOA-related matrix  $\mathbf{G}$ , it suffices to prove  $\Pi_{\Delta_0}^\perp \preceq \Pi_{\Delta_1}^\perp$ . Using Lemma 2, (C.1) and (C.2), we have

$$\begin{aligned} \Pi_{\Delta_0 \Omega}^\perp &= \Pi_{\Delta_0}^\perp = \mathbf{I} - [\Delta_1, \Delta_2] \begin{bmatrix} \Delta_1^H & \Delta_1 & \Delta_2^H & \Delta_2 \\ \Delta_2^H & \Delta_1 & \Delta_2^H & \Delta_2 \end{bmatrix}^{-1} \begin{bmatrix} \Delta_1^H \\ \Delta_2^H \end{bmatrix} \\ &\preceq \mathbf{I} - \Delta_1 (\Delta_1^H \Delta_1)^{-1} \Delta_1^H = \Pi_{\Delta_1}^\perp. \end{aligned} \quad (\text{C.3})$$

The equality holds true if and only if  $\Delta_2^H \Pi_{\Delta_1}^\perp = \mathbf{0}$ . The proof is complete.

#### APPENDIX D PROOF OF THEOREM 2

Following the settings at the beginning of Section IV-D, we can write  $\mathbf{R}_l$  as

$$\mathbf{R}_l = p \mathbf{A}_l \mathbf{A}_l^H + \mathbf{I}_M. \quad (\text{D.1})$$

In the following derivation, we shall evaluate  $\mathbf{R}_l^{-1}$  for a sufficiently large  $p$ . Since the result depends on the singularity of  $\mathbf{A}_l \mathbf{A}_l^H$ , we shall consider two different cases, i.e.,  $M \leq K$  and  $M > K$ .

If  $M \leq K$ , then  $\mathbf{A}_l \mathbf{A}_l^H$  is nonsingular. For a sufficiently large  $p$ , we can obtain the following asymptotic results by ignoring the noise-related term:

$$\mathbf{R}_l = p \mathbf{A}_l \mathbf{A}_l^H, \quad \mathbf{R}_l^{-1} = p^{-1} (\mathbf{A}_l \mathbf{A}_l^H)^{-1}. \quad (\text{D.2})$$

Substituting (D.2) into (8) gives

$$\mathbf{W}_l^H \mathbf{W}_l = p^{-2} \mathbf{O}_{1,l}, \quad \mathbf{W}_l = p^{-1} \mathbf{O}_{1,l}^{\frac{1}{2}}, \quad (\text{D.3})$$

where

$$\mathbf{O}_{1,l} = (\mathbf{A}_l^* \mathbf{A}_l^T \otimes \mathbf{A}_l \mathbf{A}_l^H)^{-1}. \quad (\text{D.4})$$

Using (D.3), we can rewrite  $\mathbf{G}$  and  $\Delta$  in (23) as

$$\mathbf{G} = \Gamma_1 \tilde{\mathbf{D}}, \quad \Delta = p^{-1} \Gamma_1 [\hat{\mathbf{D}}, \hat{\mathbf{i}}], \quad (\text{D.5})$$

where

$$\Gamma_1 = \text{blkdiag}(\mathbf{O}_{1,1}, \dots, \mathbf{O}_{1,L}). \quad (\text{D.6})$$

Substituting (D.5) into (19) yields (31), which completes the proof for this case.

If  $M > K$ ,  $\mathbf{A}_l \mathbf{A}_l^H$  is singular. We write  $\mathbf{R}_l$  in the eigen-decomposition form such that [67], [73]

$$\mathbf{R}_l = \mathbf{U}_l (p \mathbf{A}_l + \mathbf{I}_K) \mathbf{U}_l^H + \mathbf{V}_l \mathbf{V}_l^H, \quad (\text{D.7})$$

where  $\mathbf{U}_l \in \mathbb{C}^{M \times K}$  and  $\mathbf{V}_l \in \mathbb{C}^{M \times (M-K)}$  consist of normalized eigenvectors, and  $\mathbf{U}_l$  is orthogonal to  $\mathbf{V}_l$ . The diagonal matrix  $\mathbf{A}_l \in \mathbb{C}^{K \times K}$  contains the eigenvalues.

Since  $p$  is sufficiently large,  $\mathbf{I}_K$  in (D.7) can be ignored, and thus

$$\mathbf{R}_l^{-1} = p^{-1} \mathbf{U}_l \mathbf{A}_l^{-1} \mathbf{U}_l^H + \mathbf{V}_l \mathbf{V}_l^H. \quad (\text{D.8})$$

Substituting (D.8) into (8), we obtain

$$\begin{aligned} \mathbf{W}_l^H \mathbf{W}_l &= p^{-1} \mathbf{O}_{2,l} + p^{-2} \Delta_{4,l} + \mathbf{O}_{6,l}, \\ \mathbf{W}_l &= p^{-\frac{1}{2}} \mathbf{O}_{3,l} + p^{-1} \Delta_{5,l} + \mathbf{O}_{6,l}, \end{aligned} \quad (\text{D.9})$$

where

$$\begin{aligned} \mathbf{O}_{2,l} &= \mathbf{U}_l^* \mathbf{A}_l^{-1} \mathbf{U}_l^T \otimes \mathbf{V}_l \mathbf{V}_l^H + \mathbf{V}_l^* \mathbf{V}_l^T \otimes \mathbf{U}_l \mathbf{A}_l^{-1} \mathbf{U}_l^H, \\ \mathbf{O}_{3,l} &= \mathbf{U}_l^* \mathbf{A}_l^{-\frac{1}{2}} \mathbf{U}_l^T \otimes \mathbf{V}_l \mathbf{V}_l^H + \mathbf{V}_l^* \mathbf{V}_l^T \otimes \mathbf{U}_l \mathbf{A}_l^{-\frac{1}{2}} \mathbf{U}_l^H, \\ \mathbf{O}_{4,l} &= \mathbf{U}_l^* \mathbf{A}_l^{-1} \mathbf{U}_l^T \otimes \mathbf{U}_l \mathbf{A}_l^{-1} \mathbf{U}_l^H, \\ \mathbf{O}_{5,l} &= \mathbf{U}_l^* \mathbf{A}_l^{-\frac{1}{2}} \mathbf{U}_l^T \otimes \mathbf{U}_l \mathbf{A}_l^{-\frac{1}{2}} \mathbf{U}_l^H, \\ \mathbf{O}_{6,l} &= \mathbf{V}_l^* \mathbf{V}_l^T \otimes \mathbf{V}_l \mathbf{V}_l^H. \end{aligned} \quad (\text{D.10})$$

Similar to (D.6), we introduce a group of block diagonal matrices to encompass the  $L$  subbands:

$$\Gamma_w = \text{blkdiag}(\mathbf{O}_{w,1}, \dots, \mathbf{O}_{w,L}), \quad w = 2, 3, 4, 5, 6. \quad (\text{D.11})$$

Next, we present some useful results which can be verified through straightforward calculations:

$$\begin{aligned} \mathbf{D}_l^H \mathbf{O}_{w,l} &= \mathbf{O}_{w,l} \mathbf{D}_l = \mathbf{0}, \quad w = 2, 3, 6, \\ [\mathbf{D}_l, \mathbf{i}]^H \mathbf{O}_{2,l} [\mathbf{D}_l, \mathbf{i}] &= \mathbf{0}, \\ \mathbf{D}_l^H \mathbf{O}_{4,l} \mathbf{D}_l &= \mathbf{I}_K, \\ \mathbf{O}_{6,l} \tilde{\mathbf{D}}_l &= \mathbf{0}, \\ [\mathbf{D}_l, \mathbf{i}]^H \mathbf{O}_{6,l} [\mathbf{D}_l, \mathbf{i}] &= \begin{bmatrix} \mathbf{0} & \mathbf{0} \\ \mathbf{0} & M - K \end{bmatrix}. \end{aligned} \quad (\text{D.12})$$

Since the FIM is assumed to be nonsingular,  $\Delta^H \Delta$  and  $\mathbf{G}^H \Pi_{\Delta}^\perp \mathbf{G}$  are both positive definite and nonsingular. Using (D.11) and (D.12), we can express  $\Delta^H \Delta$  as

$$\Delta^H \Delta = p^{-2} \begin{bmatrix} L \mathbf{I}_K & \hat{\mathbf{D}}^H \Gamma_4 \hat{\mathbf{i}} \\ \hat{\mathbf{i}}^H \Gamma_4 \hat{\mathbf{D}} & \gamma \end{bmatrix}, \quad (\text{D.13})$$

where  $\gamma = p^2 L (M - K) + \hat{\mathbf{i}}^H \Gamma_4 \hat{\mathbf{i}}$ .

Let  $\mathbf{Y}$  and  $y$  denote the Schur complements of  $\gamma$  and  $L \mathbf{I}_K$  in (D.13), and then  $\mathbf{Y}$  and  $y$  are respectively given by

$$\begin{aligned} \mathbf{Y} &= L \mathbf{I}_K - \gamma^{-1} \hat{\mathbf{D}}^H \Gamma_4 \hat{\mathbf{i}} \hat{\mathbf{i}}^H \Gamma_4 \hat{\mathbf{D}}, \\ y &= \gamma - L^{-1} \hat{\mathbf{i}}^H \Gamma_4 \hat{\mathbf{D}} \hat{\mathbf{D}}^H \Gamma_4 \hat{\mathbf{i}}. \end{aligned} \quad (\text{D.14})$$

Then, the inverse of (D.13) can be expressed as [74]

$$(\Delta^H \Delta)^{-1} = p^2 \begin{bmatrix} \mathbf{Y}^{-1} & -\gamma^{-1} \mathbf{Y}^{-1} \hat{\mathbf{D}}^H \Gamma_4 \hat{\mathbf{i}} \\ -y^{-1} L^{-1} \hat{\mathbf{i}}^H \Gamma_4 \hat{\mathbf{D}} & y^{-1} \end{bmatrix}. \quad (\text{D.15})$$

Using (D.13) and (D.15), we can calculate  $\Pi_{\Delta}^\perp$ , and thus

$$\mathbf{G}^H \Pi_{\Delta}^\perp \mathbf{G} = \Theta_1 + \Theta_2 + \Theta_3 + \Theta_4, \quad (\text{D.16})$$

where

$$\begin{aligned} \Theta_1 &= \Gamma_5 \hat{\mathbf{D}} \mathbf{Y}^{-1} \hat{\mathbf{D}}^H \Gamma_5, \\ \Theta_2 &= -y^{-1} L^{-1} (p \Gamma_1 + \Gamma_5) \hat{\mathbf{i}} \hat{\mathbf{i}}^H \Gamma_4 \hat{\mathbf{D}} \hat{\mathbf{D}}^H \Gamma_5, \\ \Theta_3 &= -\gamma^{-1} \Gamma_5 \hat{\mathbf{D}} \mathbf{Y}^{-1} \hat{\mathbf{D}}^H \Gamma_4 \hat{\mathbf{i}} \hat{\mathbf{i}}^H (p \Gamma_6 + \Gamma_5), \\ \Theta_4 &= y^{-1} (p \Gamma_6 + \Gamma_5) \hat{\mathbf{i}} \hat{\mathbf{i}}^H (p \Gamma_6 + \Gamma_5). \end{aligned} \quad (\text{D.17})$$

Substituting (D.16) into (19) and using (D.12), we obtain

$$\mathbf{B}_{\text{uf}}^{\text{asy}} = \left[ \mathbf{Q} \tilde{\mathbf{D}}^H (p \mathbf{\Gamma}_2 + \mathbf{\Gamma}_4 - \mathbf{\Xi}_1 - \mathbf{\Xi}_2 - \mathbf{\Xi}_3 - \mathbf{\Xi}_4) \tilde{\mathbf{D}} \right]^{-1}, \quad (\text{D.18})$$

where

$$\mathbf{\Xi}_w = (p^{\frac{1}{2}} \mathbf{\Gamma}_3 + \mathbf{\Gamma}_5) \mathbf{\Theta}_w (p^{\frac{1}{2}} \mathbf{\Gamma}_3 + \mathbf{\Gamma}_5), \quad w = 1, 2, 3, 4.$$

Since  $p$  is sufficiently large,  $\{\mathbf{\Xi}_w\}_{w=1}^4$  respectively approach the following:

$$\begin{aligned} \mathbf{\Xi}_1 &= pL^{-1} \mathbf{\Gamma}_3 \mathbf{\Gamma}_5 \hat{\mathbf{D}} \hat{\mathbf{D}}^H \mathbf{\Gamma}_5 \mathbf{\Gamma}_3, \\ \mathbf{\Xi}_2 &= -L^{-2} (M - K)^{-1} \mathbf{\Gamma}_3 \mathbf{\Gamma}_6 \hat{\mathbf{i}} \hat{\mathbf{i}}^H \mathbf{\Gamma}_4 \hat{\mathbf{D}} \hat{\mathbf{D}}^H \mathbf{\Gamma}_5 \mathbf{\Gamma}_3, \\ \mathbf{\Xi}_3 &= -L^{-2} (M - K)^{-1} \mathbf{\Gamma}_3 \mathbf{\Gamma}_5 \hat{\mathbf{D}} \hat{\mathbf{D}}^H \mathbf{\Gamma}_4 \hat{\mathbf{i}} \hat{\mathbf{i}}^H \mathbf{\Gamma}_6 \mathbf{\Gamma}_3, \\ \mathbf{\Xi}_4 &= pL^{-1} (M - K)^{-1} \mathbf{\Gamma}_3 \mathbf{\Gamma}_6 \hat{\mathbf{i}} \hat{\mathbf{i}}^H \mathbf{\Gamma}_6 \mathbf{\Gamma}_3. \end{aligned} \quad (\text{D.19})$$

Finally, (32) can be obtained through the combination of (D.18) and (D.19). The proof is complete.

#### APPENDIX E PROOF OF PROPOSITION 2

We first present the proof of the asserted proposition for the case with  $\mathcal{P}_u$ . The proofs for the other three cases with  $\mathcal{P}_f$ ,  $\mathcal{P}_{\text{up}}$ , and  $\mathcal{P}_{\text{uf}}$ , respectively, follow the same idea.

For the  $l$ -th subband, we define a matrix such that  $\mathbf{\Sigma}_{u,l} \triangleq [\mathbf{D}_l \mathbf{P}_l, \mathbf{D}_l, \mathbf{i}] \in \mathbb{C}^{2K+1}$ . Note that there are  $|\mathbb{D}|$  distinct rows in  $\mathbf{\Sigma}_{u,l}$  [45]. A necessary condition for  $\mathbf{\Sigma}_{u,l}$  to have full column rank is  $K \leq (|\mathbb{D}| - 1)/2$ , which is exactly the upper bound on the resolution capacity in the narrowband scenario [45], [67]. This property is obviously inherited by each subband.

Let  $\zeta_l(k)$  and  $\delta_l(k)$  denote the  $k$ -th column in  $\mathbf{D}_l \mathbf{P}_l$  and  $\mathbf{D}_l$ , respectively. The steering vectors constructed by the nonnegative elements in  $\mathbb{D}$  are linearly independent for an arbitrary set of distinct DOAs, provided that  $K < (|\mathbb{D}| + 1)/2$  [75], which is equivalent to  $K \leq (|\mathbb{D}| - 1)/2$  for integers. This property can be generalized to the steering vectors constructed by all the elements in  $\mathbb{D}$ , under the condition that  $K \leq |\mathbb{D}| - 1$ . Therefore, it is straightforward that  $\{\zeta_l(k)\}_{k=1}^K$  and  $\{\delta_l(k)\}_{k=1}^K$  are linearly independent by themselves. The same is true for the submatrices in  $\mathbf{\Sigma}_u$ .

If  $(|\mathbb{D}| - 1)/2 < K \leq |\mathbb{D}| - 1$ , linear dependence will arise among the mixture of  $\{\delta_l(k)\}_{k=1}^K$  and  $\{\zeta_l(k)\}_{k=1}^K$ . Suppose that there exist  $u_l$  non-zero scalars  $h_1(l), \dots, h_{u_l}(l)$  and  $v_l$  non-zero scalars  $\tilde{h}_1(l), \dots, \tilde{h}_{v_l}(l)$  satisfying

$$\begin{aligned} h_1(l) \delta_l[k_1(l)] + \dots + h_{u_l}(l) \delta_l[k_{u_l}(l)] + \\ \tilde{h}_1(l) \zeta_l[k'_1(l)] + \dots + \tilde{h}_{v_l}(l) \zeta_l[k'_{v_l}(l)] = 0, \end{aligned} \quad (\text{E.1})$$

where  $1 \leq k_1(l), \dots, k_{u_l}(l), k'_1(l), \dots, k'_{v_l}(l) \leq K$  are column indices.

Notice that  $\mathbf{\Sigma}_u$  holds  $\{\mathbf{D}_l\}_{l=1}^L$  in a diagonal block, whereas  $\{\mathbf{D}_l \mathbf{P}_l\}_{l=1}^L$  are concatenated following the column direction. From (E.1), it can be deduced that linear dependence arises among the columns in  $\mathbf{\Sigma}_u$  if and only if the following factors,  $\{u_l\}_{l=1}^L$ ,  $\{v_l\}_{l=1}^L$ ,  $\{h_1(l), \dots, h_{u_l}(l)\}_{l=1}^L$ ,  $\{\tilde{h}_1(l), \dots, \tilde{h}_{v_l}(l)\}_{l=1}^L$ ,  $\{k_1(l), \dots, k_{u_l}(l)\}_{l=1}^L$ , and  $\{k'_1(l), \dots, k'_{v_l}(l)\}_{l=1}^L$ , are all independent of  $l$ . This condition is too restrictive to be satisfied for an arbitrary subband

division scheme, which means the original linear dependence among the mixture of  $\{\delta_l(k)\}_{k=1}^K$  and  $\{\zeta_l(k)\}_{k=1}^K$  can be eliminated when they are combined in  $\mathbf{\Sigma}_u$ . Therefore,  $\mathbf{\Sigma}_u$  can also have full column rank when  $(|\mathbb{D}| - 1)/2 < K \leq |\mathbb{D}| - 1$ , which violates the narrowband limitation inherited by each subband. Furthermore, it can be verified that there are  $|\mathbb{D}| L$  distinct rows in  $\mathbf{\Sigma}_u$ . Hence, a necessary condition for  $\mathbf{\Sigma}_u$  to have full column rank is  $K \leq L(|\mathbb{D}| - 1)/(L + 1)$ . The proof for the case with  $\mathcal{P}_u$  is complete.

For the case with  $\mathcal{P}_f$ , if  $K \geq M$ , linear dependence will arise among the columns in  $\mathbf{C}_l \mathbf{\Psi}$ . Similar to the previous proof, it can be demonstrated that the linear dependence among  $\{\mathbf{C}_l \mathbf{\Psi}\}_{l=1}^L$  can be eliminated when  $\{\mathbf{C}_l \mathbf{\Psi}\}_{l=1}^L$  are concatenated together following the column direction in  $\mathbf{\Sigma}_f$ . Consequently,  $\mathbf{\Sigma}_f$  can still have full column rank when  $K \geq M$ , which offers the possibility for resolving  $K \geq M$  sources.

For the case with  $\mathcal{P}_{\text{up}}$  or  $\mathcal{P}_{\text{uf}}$ , if  $K \geq |\mathbb{D}|$ , linear dependence will arise among  $\{\delta_l(k)\}_{k=1}^K$ . Notice that  $\{\xi_{l'} \mathbf{D}_{l'}\}_{l'=2}^L$  and  $\{\mathbf{D}_{l'}\}_{l'=1}^L$  are concatenated following the column direction in  $\mathbf{\Sigma}_{\text{up}}$  and  $\mathbf{\Sigma}_{\text{uf}}$ , respectively, thereby eliminating the linear dependence. As a result,  $\mathbf{\Sigma}_{\text{up}}$  and  $\mathbf{\Sigma}_{\text{uf}}$  can still have full column rank when  $K \geq |\mathbb{D}|$ , providing enhanced resolvability. The whole proof is complete.

#### REFERENCES

- [1] Y. Liang, Q. Shen, W. Cui, and W. Liu, "Cramér-Rao bound for wideband DOA estimation with uncorrelated sources," in *Proc. IEEE Global Conf. Signal Inf. Proc. (GlobalSIP)*. IEEE, 2019, pp. 1–5.
- [2] P. Stoica and A. Nehorai, "MUSIC, maximum likelihood, and Cramér-Rao bound," *IEEE Trans. Acoust., Speech, Signal Process.*, vol. 37, no. 5, pp. 720–741, 1989.
- [3] P. Stoica and A. Nehorai, "Performance study of conditional and unconditional direction-of-arrival estimation," *IEEE Trans. Acoust., Speech, Signal Process.*, vol. 38, no. 10, pp. 1783–1795, 1990.
- [4] Y. Liang, W. Liu, Q. Shen, W. Cui, and S. Wu, "A review of closed-form Cramér-Rao bounds for DOA estimation in the presence of Gaussian noise under a unified framework," *IEEE Access*, vol. 8, pp. 175 101–175 124, 2020.
- [5] G. Su and M. Morf, "Modal decomposition signal subspace algorithms," *IEEE Trans. Acoust., Speech, Signal Process.*, vol. 34, no. 3, pp. 585–602, 1986.
- [6] E. D. Di Claudio, R. Parisi, and G. Jacovitti, "Space time MUSIC: Consistent signal subspace estimation for wideband sensor arrays," *IEEE Trans. Signal Process.*, vol. 66, no. 10, pp. 2685–2699, 2018.
- [7] M. Wax, T.-J. Shan, and T. Kailath, "Spatio-temporal spectral analysis by eigenstructure methods," *IEEE Trans. Acoust., Speech, Signal Process.*, vol. 32, no. 4, pp. 817–827, 1984.
- [8] H. Wang and M. Kaveh, "Coherent signal-subspace processing for the detection and estimation of angles of arrival of multiple wide-band sources," *IEEE Trans. Acoust., Speech, Signal Process.*, vol. 33, no. 4, pp. 823–831, 1985.
- [9] B. Ottersten and T. Kailath, "Direction-of-arrival estimation for wide-band signals using the ESPRIT algorithm," *IEEE Trans. Acoust., Speech, Signal Process.*, vol. 38, no. 2, pp. 317–327, 1990.
- [10] Y. Grenier, "Wideband source location through frequency-dependent modeling," *IEEE Trans. Signal Process.*, vol. 42, no. 5, pp. 1087–1096, 1994.
- [11] M. Agrawal and S. Prasad, "DOA estimation of wideband sources using a harmonic source model and uniform linear array," *IEEE Signal Process. Lett.*, vol. 47, no. 3, pp. 619–629, 1999.
- [12] M. Agrawal and S. Prasad, "Broadband DOA estimation using "spatial-only" modeling of array data," *IEEE Trans. Signal Process.*, vol. 48, no. 3, pp. 663–670, 2000.
- [13] J. Krolik and D. Swingler, "Multiple broad-band source location using steered covariance matrices," *IEEE Trans. Acoust., Speech, Signal Process.*, vol. 37, no. 10, pp. 1481–1494, 1989.
- [14] J. Krolik and D. Swingler, "Focused wide-band array processing by spatial resampling," *IEEE Trans. Acoust., Speech, Signal Process.*, vol. 38, no. 2, pp. 356–360, 1990.

- [15] J. Krolik and D. Swingler, "The performance of minimax spatial resampling filters for focussing wide-band arrays," *IEEE Trans. Signal Process.*, vol. 39, no. 8, pp. 1899–1903, 1991.
- [16] M. A. Doron and A. J. Weiss, "On focusing matrices for wide-band array processing," *IEEE Trans. Signal Process.*, vol. 40, no. 6, pp. 1295–1302, 1992.
- [17] M. Doran, E. Doron, and A. J. Weiss, "Coherent wide-band processing for arbitrary array geometry," *IEEE Trans. Signal Process.*, vol. 41, no. 1, p. 414, 1993.
- [18] S. Valaee and P. Kabal, "Wideband array processing using a two-sided correlation transformation," *IEEE Trans. Signal Process.*, vol. 43, no. 1, pp. 160–172, 1995.
- [19] E. D. Di Claudio and R. Parisi, "WAVES: Weighted average of signal subspaces for robust wideband direction finding," *IEEE Trans. Signal Process.*, vol. 49, no. 10, pp. 2179–2191, 2001.
- [20] F. Sellone, "Robust auto-focusing wideband DOA estimation," *Signal Process.*, vol. 86, no. 1, pp. 17–37, 2006.
- [21] P. M. Schultheiss and H. Messer, "Optimal and suboptimal broad-band source location estimation," *IEEE Trans. Signal Process.*, vol. 41, no. 9, pp. 2752–2763, 1993.
- [22] M. A. Doron, A. J. Weiss, and H. Messer, "Maximum-likelihood direction finding of wide-band sources," *IEEE Trans. Signal Process.*, vol. 41, no. 1, p. 411, 1993.
- [23] P.-J. Chung, M. L. Jost, and J. F. Böhme, "Estimation of seismic-wave parameters and signal detection using maximum-likelihood methods," *Computers & Geosciences*, vol. 27, no. 2, pp. 147–156, 2001.
- [24] J. C. Chen, R. E. Hudson, and K. Yao, "Maximum-likelihood source localization and unknown sensor location estimation for wideband signals in the near-field," *IEEE Trans. Signal Process.*, vol. 50, no. 8, pp. 1843–1854, 2002.
- [25] P. Pal and P. Vaidyanathan, "Nested arrays: A novel approach to array processing with enhanced degrees of freedom," *IEEE Trans. Signal Process.*, vol. 58, no. 8, pp. 4167–4181, 2010.
- [26] P. P. Vaidyanathan and P. Pal, "Sparse sensing with co-prime samplers and arrays," *IEEE Trans. Signal Process.*, vol. 59, no. 2, pp. 573–586, 2011.
- [27] S. Qin, Y. D. Zhang, and M. G. Amin, "Generalized coprime array configurations for direction-of-arrival estimation," *IEEE Trans. Signal Process.*, vol. 63, no. 6, pp. 1377–1390, 2015.
- [28] P. Pal and P. P. Vaidyanathan, "Coprime sampling and the MUSIC algorithm," in *Proc. Digital Signal Process. Workshop and IEEE Signal Process. Educ. Workshop (DSP/SPE)*. IEEE, 2011, pp. 289–294.
- [29] M. Guo, Y. D. Zhang, and T. Chen, "DOA estimation using compressed sparse array," *IEEE Trans. Signal Process.*, vol. 66, no. 15, pp. 4133–4146, 2018.
- [30] C.-L. Liu and P. Vaidyanathan, "Super nested arrays: Linear sparse arrays with reduced mutual coupling—Part I: Fundamentals," *IEEE Trans. Signal Process.*, vol. 64, no. 15, pp. 3997–4012, 2016.
- [31] A. Raza, W. Liu, and Q. Shen, "Thinned coprime array for second-order difference co-array generation with reduced mutual coupling," *IEEE Trans. Signal Process.*, vol. 67, no. 8, pp. 2052–2065, 2019.
- [32] Q. Shen, W. Liu, W. Cui, S. Wu, and P. Pal, "Simplified and enhanced multiple level nested arrays exploiting high-order difference co-arrays," *IEEE Trans. Signal Process.*, vol. 67, no. 13, pp. 3502–3515, 2019.
- [33] Q. Shen, W. Liu, W. Cui, and S. Wu, "Extension of co-prime arrays based on the fourth-order difference co-array concept," *IEEE Signal Process. Lett.*, vol. 23, no. 5, pp. 615–619, 2016.
- [34] Y. D. Zhang, M. G. Amin, and B. Himed, "Sparsity-based DOA estimation using co-prime arrays," in *Proc. IEEE Int. Conf. Acoust., Speech, Signal Process. (ICASSP)*. IEEE, 2013, pp. 3967–3971.
- [35] H. Qiao and P. Pal, "On maximum-likelihood methods for localizing more sources than sensors," *IEEE Signal Process. Lett.*, vol. 24, no. 5, pp. 703–706, 2017.
- [36] K. Han and A. Nehorai, "Wideband Gaussian source processing using a linear nested array," *IEEE Signal Process. Lett.*, vol. 20, no. 11, pp. 1110–1113, 2013.
- [37] J. Liu, Y. Lu, Y. Zhang, and W. Wang, "Fractional difference co-array perspective for wideband signal doa estimation," *EURASIP J. Adv. Signal Process.*, vol. 2016, no. 133, pp. 1–12, 2016.
- [38] Q. Shen, W. Liu, W. Cui, S. Wu, Y. D. Zhang, and M. G. Amin, "Low-complexity direction-of-arrival estimation based on wideband co-prime arrays," *IEEE/ACM Trans. Audio, Speech, Language Process.*, vol. 23, no. 9, pp. 1445–1453, 2015.
- [39] Q. Shen, W. Liu, W. Cui, S. Wu, Y. D. Zhang, and M. G. Amin, "Wideband DOA estimation for uniform linear arrays based on the co-array concept," in *Proc. Eur. Signal Process. Conf. (EUSIPCO)*. IEEE, 2015, pp. 2835–2839.
- [40] Q. Shen, W. Cui, W. Liu, S. Wu, Y. D. Zhang, and M. G. Amin, "Underdetermined wideband DOA estimation of off-grid sources employing the difference co-array concept," *Signal Process.*, vol. 130, pp. 299–304, 2017.
- [41] Q. Shen, W. Liu, W. Cui, and S. Wu, "Underdetermined DOA estimation under the compressive sensing framework: A review," *IEEE Access*, vol. 4, pp. 8865–8878, 2016.
- [42] H. Wu, Q. Shen, W. Liu, and W. Cui, "Underdetermined low-complexity wideband DOA estimation with uniform linear arrays," in *Proc. Sensor Array Multichannel Signal Process. Workshop (SAM)*, 2020, pp. 1–5.
- [43] H. Messer, "The potential performance gain in using spectral information in passive detection/localization of wideband sources," *IEEE Trans. Signal Process.*, vol. 43, no. 12, pp. 2964–2974, 1995.
- [44] J. P. Ianniello, "High-resolution multipath time delay estimation for broad-band random signals," *IEEE Trans. Acoust., Speech, Signal Process.*, vol. 36, no. 3, pp. 320–327, 1988.
- [45] A. Koochakzadeh and P. Pal, "Cramér-Rao bounds for underdetermined source localization," *IEEE Signal Process. Lett.*, vol. 23, no. 7, pp. 919–923, 2016.
- [46] A. J. Ficker and Y. Bresler, "Sensor-efficient wideband source location," in *Proc. Midwest Symp. Circuits Syst.* IEEE, 1989, pp. 586–589.
- [47] H.-S. Hung and M. Kaveh, "Fisher information matrix of the coherently averaged covariance matrix," *IEEE Trans. Signal Process.*, vol. 39, no. 6, pp. 1433–1435, 1991.
- [48] D. N. Swingler, "An approximate expression for the Cramér-Rao bound on DOA estimates of closely spaced sources in broadband line-array beamforming," *IEEE Trans. Signal Process.*, vol. 42, no. 6, pp. 1540–1543, 1994.
- [49] M. A. Doron and E. Doron, "Wavefield modeling and array processing. Part III. Resolution capacity," *IEEE Trans. Signal Process.*, vol. 42, no. 10, pp. 2571–2580, 1994.
- [50] M. A. Hasan, M. R. Azimi-Sadjadi, and G. J. Dobeck, "Separation of multiple time delays using new spectral estimation schemes," *IEEE Trans. Signal Process.*, vol. 46, no. 6, pp. 1580–1590, 1998.
- [51] K. Buckley, "Spatial/spectral filtering with linearly constrained minimum variance beamformers," *IEEE Trans. Acoust., Speech, Signal Process.*, vol. 35, no. 3, pp. 249–266, 1987.
- [52] Q. Shen, W. Liu, W. Cui, S. Wu, Y. D. Zhang, and M. G. Amin, "Focused compressive sensing for underdetermined wideband DOA estimation exploiting high-order difference coarrays," *IEEE Signal Process. Lett.*, vol. 24, no. 1, pp. 86–90, 2016.
- [53] D. Tse and P. Viswanath, *Fundamentals of Wireless Communication*. New York, NY, USA: Cambridge University Press, 2005.
- [54] B. Elie, J. Yong, A. Fauzia, and G. A. Moeness, "Multi-frequency co-prime arrays for high-resolution direction-of-arrival estimation," *IEEE Trans. Signal Process.*, vol. 63, no. 14, pp. 3797–3808, 2015.
- [55] F. Wang, Z. Tian, J. Fang, and G. Leus, "Wideband direction of arrival estimation with sparse linear arrays," in *Proc. IEEE Int. Conf. Acoust., Speech, Signal Process. (ICASSP)*, 2020, pp. 4542–4546.
- [56] Y. Bresler, "On the resolution capacity of wideband sensor arrays: Further results," in *Proc. IEEE Int. Conf. Acoust., Speech, Signal Process. (ICASSP)*. IEEE, 1991, pp. 1353–1356.
- [57] M. Wang and A. Nehorai, "Coarrays, MUSIC, and the Cramér-Rao bound," *IEEE Trans. Signal Process.*, vol. 65, no. 4, pp. 933–946, 2017.
- [58] P. Stoica and R. L. Moses, *Spectral Analysis of Signals*. Upper Saddle River, NJ, USA: Pearson Prentice Hall, 2005.
- [59] B. Ottersten, M. Viberg, P. Stoica, and A. Nehorai, "Exact and large sample maximum likelihood techniques for parameter estimation and detection in array processing," in *Radar Array Process.* Springer, 1993, pp. 99–151.
- [60] D. R. Brillinger, *Time Series: Data Analysis and Theory*. Philadelphia, PA, USA: Society for Industrial and Applied Mathematics, 2001.
- [61] F. J. Harris, "On the use of windows for harmonic analysis with the discrete Fourier transform," *Proc. IEEE*, vol. 66, no. 1, pp. 51–83, 1978.
- [62] S. Sando, A. Mitra, and P. Stoica, "On the Cramér-Rao bound for model-based spectral analysis," *IEEE Signal Process. Lett.*, vol. 9, no. 2, pp. 68–71, 2002.
- [63] D. Slepian, "Estimation of signal parameters in the presence of noise," *Trans. IRE Prof. Group Inf. Theory*, vol. 3, no. 3, pp. 68–89, 1954.
- [64] W. J. Bangs, "Array Processing with Generalized Beamformers," Ph.D. dissertation, Yale Univ., New Haven, CT, 1971.
- [65] H. L. Van Trees, *Optimum Array Processing: Part IV of Detection, Estimation, and Modulation Theory*. New York, NY, USA: John Wiley & Sons, 2004.
- [66] P. Stoica, E. G. Larsson, and A. B. Gershman, "The stochastic CRB for array processing: A textbook derivation," *IEEE Signal Process. Lett.*, vol. 8, no. 5, pp. 148–150, 2001.

- [67] C.-L. Liu and P. Vaidyanathan, "Cramér-Rao bounds for coprime and other sparse arrays, which find more sources than sensors," *Digital Signal Process.*, vol. 61, pp. 43–61, 2017.
- [68] B. Hochwald and A. Nehorai, "On identifiability and information-regularity in parametrized normal distributions," *Circuits, Syst., Signal Process.*, vol. 16, no. 1, pp. 83–89, 1997.
- [69] P. Stoica and T. L. Marzetta, "Parameter estimation problems with singular information matrices," *IEEE Trans. Signal Process.*, vol. 49, no. 1, pp. 87–90, 2001.
- [70] W. Suleiman, P. Parvazi, M. Pesavento, and A. M. Zoubir, "Non-coherent direction-of-arrival estimation using partly calibrated arrays," *IEEE Trans. Signal Process.*, vol. 66, no. 21, pp. 5776–5788, 2018.
- [71] W. Cui, Q. Shen, W. Liu, and S. Wu, "Low complexity DOA estimation for wideband off-grid sources based on re-focused compressive sensing with dynamic dictionary," *IEEE J. Sel. Topics Signal Process.*, vol. 13, no. 5, pp. 918–930, 2019.
- [72] R. A. Horn, R. A. Horn, and C. R. Johnson, *Matrix Analysis*. New York, NY, USA: Cambridge University Press, 1990.
- [73] M. Jansson, B. Goransson, and B. Ottersten, "A subspace method for direction of arrival estimation of uncorrelated emitter signals," *IEEE Trans. Signal Process.*, vol. 47, no. 4, pp. 945–956, 1999.
- [74] H. Lütkepohl, *Handbook of Matrices*. Chichester, West Sussex, UK: John Wiley & Sons, 1996.
- [75] Y. I. Abramovich, N. K. Spencer, and A. Y. Gorokhov, "Resolving manifold ambiguities in direction-of-arrival estimation for nonuniform linear antenna arrays," *IEEE Trans. Signal Process.*, vol. 47, no. 10, pp. 2629–2643, 1999.



**Yibao Liang** was born in Shandong, China, in 1994. He received his B.Eng and BBA. degrees from Beijing Institute of Technology, Beijing, China, in 2016, where he is currently pursuing the Ph.D. degree with the School of Information and Electronics. From October 2019 to March 2020, he was a Visiting Researcher with the Department of Electronic and Electrical Engineering, University of Sheffield, Sheffield, UK. His research interests include radar and array signal processing.



**Wei Cui** received the B.S. degree in physics and Ph.D. degree in Electronics Engineering from Beijing Institute of Technology, Beijing, China, in 1998 and 2003, respectively. From March 2003 to March 2005, he worked as a Post-Doctor in the School of Electronic and Information Engineering, Beijing Jiaotong University. Since then, he has been with the Beijing Institute of Technology, where he is currently a Professor with the School of Information and Electronics. His research interests include adaptive signal processing, array signal processing, sparse signal processing, and their various applications such as Radar, aerospace telemetry tracking and command. He has published more than 100 papers, holds 52 patents, and received the Ministerial Level Technology Advancement Award twice.



**Qing Shen** received his B.S. degree in 2009 and Ph.D. degree in 2016, both from the Beijing Institute of Technology, Beijing, China. He then worked as a Postdoctoral Researcher with the Beijing Institute of Technology, where he is currently an Associate Professor. From 2013 to 2015 and from 2018 to 2019, he was a Sponsored Researcher in the Department of Electronic and Electrical Engineering, University of Sheffield, Sheffield, UK. His research interests include sensor array signal processing, statistical signal processing, adaptive signal processing, and their various applications such as acoustics, radar, sonar, and wireless communications. He was the recipient of two Excellent Ph.D. Thesis Awards from both the Chinese Institute of Electronics and the Beijing Institute of Technology in 2016. He was also the recipient of the Second-Class Prize of the National Award for Technological Invention in 2020, the First-Class Prize of the Science and Technology (Technological Invention) Award from the Chinese Institute of Electronics in 2018, the Second-Class Prize of the Ministerial Level Science and Technology Progress Award in 2014, and the Young Scientist Award from the IEEE ICET 2021. He is currently a member of the Digital Signal Processing Technical Committee of the IEEE Circuits and Systems Society. He is the Financial Co-Chair of the IEEE CAMSAP 2021 (which will be postponed to 2023 due to the uncertainty generated by the pandemic), Special Session Co-Organizer of the ICCAIS 2021. He served as the Session Co-Chair of the IEEE ISCAS 2021, and the Guest Editor for the IJAP in 2020.



**Wei Liu** (S'01-M'04-SM'10) received his BSc and LLB. degrees from Peking University, China, in 1996 and 1997, respectively, MPhil from the University of Hong Kong in 2001, and PhD from the School of Electronics and Computer Science, University of Southampton, UK, in 2003. He then worked as a postdoc first at Southampton and later at the Department of Electrical and Electronic Engineering, Imperial College London. Since September 2005, he has been with the Department of Electronic and Electrical Engineering, University of Sheffield, UK, first as a Lecturer and then a Senior Lecturer. He has published more than 300 journal and conference papers, five book chapters, and two research monographs titled "Wideband Beamforming: Concepts and Techniques" (John Wiley, March 2010) and "Low-Cost Smart Antennas" (by Wiley-IEEE, March 2019), respectively. His research interests cover a wide range of topics in signal processing, with a focus on sensor array signal processing and its various applications, such as robotics and autonomous systems, human computer interface, radar, sonar, satellite navigation, and wireless communications.

He is a member of the Digital Signal Processing Technical Committee of the IEEE Circuits and Systems Society (Secretary from May 2020) and the Sensor Array and Multichannel Signal Processing Technical Committee of the IEEE Signal Processing Society (Chair from Jan 2021). He was an Associate Editor for *IEEE Trans. on Signal Processing* (2015-2019) and *IEEE Access* (2016-2021), and is currently an editorial board member of the journal *Frontiers of Information Technology and Electronic Engineering* and the *Journal of The Franklin Institute*.



**Siliang Wu** received his Ph.D. degree in Electrical Engineering from Harbin Institute of Technology in 1995. He then worked as a post-doctor, and is now a professor in Beijing Institute of Technology. His current research interests include statistical signal processing, sensor array and multichannel signal processing, adaptive signal processing and their applications in radar, aerospace TT&C and satellite navigation. He has authored and co-authored more than 300 journal papers and holds 72 patents. He received the first-class prize of the National Award for Technological Invention, and the Ho Leung Ho Lee Foundation Prize in 2014. He is also the recipient of the State Council Special Allowance, the National Model Teacher, the National May 1 Labor Medal, and the National Outstanding Scientific and Technological Personnel.